Energy, Mines and Resources Canada | Énergie, Mines et Ressources Canada

CANMET

Canada Centre for Mineral and Energy Technology | Centre canadien de la technologie des minéraux et de l'énergie

TOUGHNESS OF WELD METALS FOR FABRICATION OF COLD MARINE STRUCTURES AND VESSELS

PART 2: SUBMERGED ARC WELDING

J.E.M. Braid and J.A. Gianetto

APRIL 1988

...document is to be cited ... previously ... with the permission ... the Canada ... Mineral and Energy Technology (CANMET)

Ce document ... Énergie (CANMET)

This programme was funded by the Federal Panel on Energy R&D (PERD)

33 pp

METALS TECHNOLOGY LABORATORIES
(formerly PHYSICAL METALLURGY RESEARCH LABORATORIES)

REPORT: MTL 88-25(TR)

MICROMEDIA

88-04998/

METALS TECHNOLOGY LABORATORIES
REPORT: MTL 88-25(TR)

TOUGHNESS OF WELD METALS FOR FABRICATION OF COLD MARINE STRUCTURES AND VESSELS

PART 2: SUBMERGED ARC WELDING

by

J.E.M. Braid and J.A. Gianetto

ABSTRACT

A series of twelve butt welds in 20 mm thick C-Mn microalloyed structural steel plate has been made using wire/flux combinations chosen from European and North American manufacturers specializing in submerged arc welding for critical applications. Basic fluxes were selected along with wires, recommended by the manufacturer, of C-Mn, C-Mn-Ni, C-Mn-Ti-B and C-Mn-Mo compositions. The welds were evaluated in terms of microstructure and toughness. Ten of the twelve welds tested met a 0.08 mm CTOD requirement at -30°C while two of the welds met a 0.2 mm CTOD requirement at -30°C. In general the submerged arc welds showed better toughness than comparable shielded-metal-arc welds.

Low temperature fracture of the welds occurred by cleavage initiating from large, >1 μm diam inclusions primarily in grain boundary ferrite. Poor toughness was associated with welds with high inclusion volume fractions, high numbers of large inclusions and/or low amounts of acicular ferrite microstructures. The highest proportions of acicular ferrite were associated with additions of 0.01-0.03% Ti, 0.001-0.003% B and/or 0.25% Mo. Further optimization of weld metals with 2-3% Ni additions is required if known improvements in cleavage resistance of ferrite are to be exploited.

LABORATOIRES DE LA TECHNOLOGIE DES MÉTAUX
RAPPORT: MTL 88-25(TR)

TÉNACITÉ DES MÉTAUX DE SOUDURE DESTINÉS A LA FABRICATION DES STRUCTURES MARITIMES ET NAVIRES POUR RÉGIONS FROIDES PARTIE 2 : SOUDAGE À L'ARC SOUS FLUX

par

J.E.M. Braid et J.A. Gianetto

RÉSUMÉ

On a effectué une série de douze soudages bout à bout dans une tôle d'acier structural microallié C-Mn de 20 mm d'épaisseur, en employant des combinaisons fil-flux de soudage choisies chez des fabricants européens et nord-américains spécialisés dans le soudage à l'arc sous flux, pour applications dans des conditions critiques. En même temps que les fils de soudage, on a choisi des flux basiques recommandés par le fabricant, ayant les compositions suivantes: C-Mn, C-Mn-Ni, C-Mn-Ti-B et C-Mn-Mo. On a évalué les soudures en fonction de leur microstructure et de leur ténacité. Dix des douze soudures testées ont satisfait à une norme de 0,08 mm pour le déplacement de l'ouverture de la pointe des fissures (CTOD) à -30°C; deux de ces soudures ont satisfait à une norme CTOD de 0,2 mm à -30°C. En général, les soudures effectuées à l'arc sous flux ont présenté une meilleure ténacité que des soudures comparables faites à l'arc métallique avec électrode enrobée.

Les fractures des soudures effectuées à basse température avaient pour origine le clivage survenant à partir de grandes inclusions, > 1 µm de diamètre, surtout présentes dans la ferrite de la périphérie des grains. On a associé une faible ténacité aux soudure caractérisées par une forte fraction volumétrique d'inclusions, et par un nombre important de grandes inclusions et/ou de faibles quantités de microstructures ferrites aciculaires. Les proportions les plus élevées de ferrite aciculaire étaient associées à des ajouts de 0,01-0,03% Ti, 0,001-0,003% B et/ou 0,25% Mo. Il faut encore optimiser la composition des métaux de soudure avec des ajouts de 2-3% de Ni, si l'on veut exploiter les améliorations connues de la résistance de la ferrite au clivage.

INTRODUCTION

Over the past two decades the submerged-arc welding process has seen increased utilization for welding in critical applications owing to the inherent productivity and superior weld-metal mechanical properties which can be achieved by this process. Several investigations have focused on improving weld-metal toughness by optimizing the microstructure via modifications to the weld-metal composition and/or inclusion volume fraction and size distribution (1-6). It is generally agreed upon that improved resistance to brittle fracture at low temperatures coincides with a high proportion of fine-grained acicular ferrite. Much of the welding technology developed for critical applications such as the fabrication of offshore structures has been developed for North Sea installations. Few studies have evaluated low temperature, <-10°C, weld-metal fracture toughness which will be required for applications typical of offshore structures and Arctic vessels for Canada's East Coast and Arctic regions. The environmental conditions of Canada's East Coast regions are quite severe with low design temperatures (-17 to -20°C), sea ice, and the presence of icebergs. Design criteria for the Beaufort Sea and Arctic regions present further challenges with temperatures as low as -50°C and pack ice representing the main design obstacles. A need exists, therefore, to develop welding technology which can meet the design criterion for the fabrication of offshore structures and Arctic Vessels. In Part 1 of the programme the evaluation of the fracture toughness of shielded-metal-arc weld metals deposited using a range of currently available consumables was reported (7). The aim of the present study was to evaluate the fracture toughness of submerged-arc welds (SAW) deposited with a range of wire/flux combinations designed for critical applications.

EXPERIMENTAL

Materials and Welding Procedure

A 20 mm thick microalloyed C-Mn-Ni-Nb-V steel (Table 1) conforming to CSA G40.21-350WT specification was selected for the experimental programme. The plates were produced using controlled-rolling and fine-grain practice.

Welding consumables (wire/flux combinations) were chosen from manufacturers specializing in submerged-arc welding for critical applications. In general,basic fluxes were selected along with wires of C-Mn, C-Mn-Ni, C-Mn-Ti-B and C-Mn-Mo chemical compositions. Table 2 lists the corresponding weld identification. The welding parameters were optimized by making bead-on-plate (BOP) trial welds to maintain a nominal heat input of 2.8 kJ/mm (Table 3). The joint design consisted of a single-vee preparation with a 60° included angle and a 6 mm land. A pass sequence which maximized the amount of as-deposited weld metal was employed as shown in Fig. 1. Backgouging, by the carbon arc process, was employed prior to deposition of the final back pass. The portion of each weld used for tensile and CTOD specimens was given a hydrogen removal heat-treatment (93°C for 24 h).

Mechanical Testing

All weld-metal-tensile, Charpy-V-notch and full-section thickness (B x 2B) CTOD specimens were machined from each weldment. Charpy and CTOD specimens were removed transverse to the weld length and notched through-thickness at the weld centerline. The Charpy specimens were located at the weld mid-thickness (t/2) position. Transition curves were generated for each weld (based on an average of three tests) by impact testing at temperatures within the range of -80°C to 20°C.

All CTOD specimens were locally compressed below the machined notch prior to fatigue cracking to a targeted crack length to specimen width ratio (a/W) of 0.45 to 0.55. The tests were conducted at -10°C and -30°C in accordance with British Standard BS5762 1979.

Metallography and Fractography

Standard metallographic techniques were used to prepare cross-sections from each weld. The percentage of weld-metal regions (as-deposited, coarse-grain reheated and fine-grain reheated) were quantified along the weld centerline using a light microscope. Optical microscopy was used to characterize the weld-metal microstructures. Point counting was performed on the last as-deposited bead following the current IIW classification scheme (8). The currently used nomenclature lists the following microstructural constituents; acicular ferrite (AF), grain boundary ferrite (GF), ferrite with

second phase (FS) and polygonal ferrite (PF). Selected CVN and CTOD fracture surfaces were examined in a scanning electron microscope (SEM) in order to determine the mode and origins of fracture.

RESULTS

Chemical Composition

The chemical compositions and relative hardenabilities as expressed by various carbon equivalent formulae are presented in Tables 4 and 5. The alloy additions come principally from the wire while the residual alloying elements i.e., V and Nb result from dilution with the base material and are essentially the same for all welds. The major contributions to hardenability in the case of the C-Mn welds comes from the alloy additions of C, Mn, Si and to a lesser degree Ni. The C, Si and Ni were similar for all these welds, whereas Mn varied from 1.33% to 1.50% depending on the electrode specification e.g. AWS EM12K or EH14. With regards to Mn content several reports have shown that the optimum Mn level of 1.4% promotes the formation of acicular ferrite and thus increases the resistance to cleavage fracture (9). Weld SA 9 contained a high level of Ti and B even though the wire/flux combination was specified as a C-Mn variety.

In the C-Mn-1 Ni welds C, Mn, Si and Ni are considered the most significant contributors to weld-metal hardenability. The carbon level was similar for these welds; however, the Mn varied from 1.28 to 1.43% and the Si was within the range 0.27 to 0.38%. Weld metal nickel contents varied from 0.550 for weld SA 7 to 0.700 for weld SA 5. These levels were somewhat lower than the nominal 1% Ni specified for these electrodes. Chromium and Mo levels were very low and considered to be diluted from the base material. The Ti and B levels observed in these welds were considered to be unintentional and resulted from dilution.

The primary elements of the higher Ni welds (C-Mn-2-3 Ni); C, Mn, Si, Ni and Mo, varied relative to each other. A balance of elements particularly Mn, Ni and Mo is necessary in order to achieve the required strength levels i.e., 550 MPa. Therefore, in general the Mn content is lower ($\sim$1.25%) than in the C-Mn-1 Ni welds ($\sim$1.40%) and Mo may or may not be added. The Si contents of welds SA 6 and SA 8 were slightly lower than the C-Mn-1 Ni welds.

The Ni levels were again lower than the nominal compositional specification for the respective welding wires. The Mo levels of weld SA 6 was higher than all the other Ni welds suggesting it was added to increase strength.

In the case of welds SA 3 and SA 10 the principal alloy additions of Mn, Si, Ni, Ti, B, and Mo are seen to differ. The Mn varied from 1.25% (SA 3) to 1.60 (SA 10) while the Si ranged from 0.205 for SA 3 and 0.306 for SA 10. The Ni levels were only slightly different, whereas, the Ti-B and Mo levels are much lower in weld SA 3.

The effectiveness of Ti-B additions to weld metals via the electrode, flux or both have been studied for their ability to promote acicular ferrite microstructures (3,10-13).

For the C-Mn-Mo weld, SA 12, the alloy additions of C, Mn, Si, Ni and particularly Mo contribute to the weld metal hardenability. Work by Ito and Nakanishi (4) has shown that Mo contents $\leq$0.3% promote acicular ferrite, whereas, higher levels tended to form side-plate (ferrite with second phase). The C, Mn, Si and Ni contents are essentially optimized for this weld metal.

The variation in the remaining elements of each weld, particularly, Cr, Cu and Al is principally due to the various wire/flux chemistries.

Because all welds were made with basic type fluxes, with the exception of welds SA 9 and SA 10, the oxygen contents were within the range of 200-300 ppm. Welds SA 9 and SA 10 had higher levels of 365 and 474 ppm, respectively. The nitrogen contents of all welds were less than 95 ppm which is considered normal for SA welding.

Mechanical Properties

Tensile

The tensile properties for the welds are shown in Table 6. The yield strengths are shown to vary from 500 MPa to 599 MPa with a variation in ultimate strength from 625 MPa to 697 MPa. However, it is noted that weld SA 10 had the highest strength (599 MPa yield, 697 MPa tensile) with all other welds between 500 MPa and 559 MPa yield and 625 MPa and 687 MPa ultimate. Only one weld had an elongation below 24%, SA 8 at 21%. Hence all the welds, with perhaps the exception of SA 8 (21% elongation), meet the same tensile requirements as E550XX-X SMAW electrode in the as-welded condition.

Notch Toughness Properties

The Charpy impact transition curves generated for the welds based on the average of three tests per temperature are shown in Fig. 2, 3, 4, and 5. The 35 J transition temperatures and impact energies at 20°C are presented in Table 7.

For the C-Mn welds, Fig. 2, the resistance to cleavage fracture was assessed by comparing the 35 J temperatures (Table 7). It can be seen that there was little difference in notch toughness for welds SA 4, SA 9 and SA 11. Weld SA 1 exhibited a higher 35 J temperature (-26°C) compared with the others (~32-34°C).

The transition curves for the C-Mn-Ni welds, shown in Fig. 3 and 4, indicate an overall improvement in toughness for all welds except weld SA 8, made using a nominally 2% Ni electrode wire. Weld SA 8 exhibited the highest 35 J temperature (-13°C), while weld SA 7 achieved the lowest (-47°C).

The Charpy results for the Ti-B-Mo and Mo welds (SA 3, SA 10 and SA 12) are shown in Fig. 5. The low temperature toughness was significantly better for these welds in comparison with the C-Mn or C-Mn-Ni weld deposits. Weld SA 10 achieved a 35 J temperature of -58°C, while welds SA 3 and SA 12 exhibited 35 J temperatures of less than -60°C. The shelf energy of 191 J achieved by weld SA 3 was 66 J higher than weld SA 10 for tests conducted at 20°C. This difference can be related to the O + S content of each weld (SA 3 = 0.036%, SA 10 = 0.058%). Weld SA 12 had not reached its upper shelf limit and therefore exhibited lower toughness at 20°C.

Fracture Toughness (CTOD)

The results of the CTOD test are presented in Table 8. As in the previous study on shielded-metal-arc welds (7) a CTOD requirement of 0.08 mm for the 20 mm thick welds was established using the proposed revisions to the U.K. Dept. of Energy Guidance Notes for offshore structures (22). All welds, except SA 5 and SA 8 tested at -30°C, met the 0.08 mm requirement at -30°C and -10°C.

In general, fracture toughness increases with increasing test temperature (-30°C to -10°C). Also, the test values display a large amount of scatter ranging from 0.023 mm to 0.645 mm. The C-Mn welds were all above 0.08 mm at both test temperatures with weld SA 1 showing the best toughness

followed by SA 4, SA 11 and SA 9. One of the C-Mn-1 Ni welds, SA 5, has a low value of 0.069 mm at -30°C. Weld SA 2 had a low value of 0.081 mm and a value of 0.231 mm at -30°C with all other values above 0.47 mm. Weld SA 2 was considered to have the best fracture toughness of the C-Mn-1 Ni group followed by SA 7 and SA 5.

Weld SA 8 of the C-Mn-2/3 Ni group showed the poorest fracture toughness of all 12 welds with three values, at -30°C, below 0.08 mm, and all values below 0.2 mm. Weld SA 3 of the C-Mn-Ti-B group showed the best fracture toughness of all 12 welds tested with one value of 0.218 mm at -30°C and all others above 0.56 mm. Weld SA 10, the other C-Mn-Ti-B weld, had the second poorest fracture toughness of all 12 welds. Weld SA 12, the C-Mn-Mo weld, had the third best overall fracture toughness.

Microstructure

The general macrostructure in the vicinity of the CTOD crack front, located at the weld centerline, is shown typically in Fig. 6. The structure was composed of a very large proportion of as-deposited (columnar) weld metal with varying amounts of reheated weld-metal regions. The proportions of as-deposited and reheated weld-metal regions are listed in Table 9 for the full-plate thickness, the Charpy location, and the central one-third for each weldment. All welds contained approximately 90% as-deposited weld metal for the full-plate thickness, with the exception of weld SA 8 which contained 80%. In general, all welds, except welds SA 8 and SA 9, had at least 80% as-deposited columnar weld metal in the Charpy location. The percentage of as-deposited weld metal decreased within the central one-third region, however, only weld SA 8 contained less than 68% as-deposited weld metal. Several welds were composed of $\geq$75% as-deposited weld metal within this region. The observed variation of the percentages of as-deposited and reheated regions can be attributed to the inherent operating characteristics of the individual wire/flux combinations which resulted in slight differences in pass sequences.

The results of the quantitative analysis performed by point counting on the last as-deposited weld bead are presented in Table 10. There are wide variations in the percentage of microstructural constituents between welds of different nominal compositions, however, the variations were less within a given group. The microstructure of a given weld is dependant on several factors such as, the chemical composition, type and size distribution of

inclusions, austenite grain size and weld thermal history. Since the same nominal heat input (thermal cycle) was used the variations can be attributed to the remaining factors.

Representative micrographs of the as-deposited (columnar) structure are shown in Fig. 7 to 10. Specific microstructural constituents are indicated in Fig. 7(b) and 9(b). Generally, the microstructure of the C-Mn welds was composed of an acicular ferrite matrix delineated by grain boundary ferrite and ferrite with second phase. The amounts of acicular ferrite varied from 55% to 62% for welds SA 9, and SA 4 and SA 11 respectively, balanced with varying amounts of grain boundary ferrite and ferrite with second phase (Fig. 7(a)-(d)). For the C-Mn-1 Ni welds (Fig. 8), there was an increase in the percentage of acicular ferrite at the expense of grain boundary ferrite and ferrite with second phase. Weld SA 2 contained the highest proportion, 68%, of acicular ferrite. In the case of the C-Mn-2-3 Ni welds, SA 6 and SA 3 (Fig. 9), there was a significant increase in the percentage of ferrite with second phase at the expense of acicular ferrite for weld SA 8, whereas, weld SA 6 contained 60% acicular ferrite, similar to the C-Mn-1 Ni welds. Photomicrographs of the C-Mn-Ti-B welds are shown in Fig. 10(a) and (b). There was a significant increase in the percentage of acicular ferrite, $\geq$75%, at the expense of grain boundary ferrite. Weld SA 10 contained less grain boundary ferrite (12%) compared with weld SA 3 (20%).

The C-Mn-Mo weld, SA 12, (Fig. 10(c)), contained the highest percentage of acicular ferrite (85%) and less prevalent grain boundary ferrite veins compared with all the other welds.

The variations in microstructure for all the weldments can be attributed to the differences in weld-metal chemical composition including oxygen content. Oxygen is found primarily in the form of non-metallic inclusions which influence acicular ferrite nucleation (6,14-21).

The microstructures of the coarse and fine-grain reheated weld metal regions are shown typically in Fig. 11. The coarse-grain reheated region resembled the as-deposited structure, the only difference being that the prior austenite grains were equiaxed. The fine-grain reheated region consisted of polygonal ferrite with varying amounts of carbide aggregate for all welds.

DISCUSSION

Tensile Properties

The tensile properties shown in Table 6 are basically similar for all 12 welds. All the welds have similar chemistries (Table 4) with the exception of the specific alloy additions within each group. Additions of Ni were, in general, balanced by decreases in Mn which leads to all welds having similar carbon equivalents (Table 5) and similar hardenability. The welds also had similar microstructures with the exception of SA 8 which had only 40% acicular ferrite; all other welds had 50% or more acicular ferrite.

The higher strength of weld SA 10 occurs as a result of its higher Mn content (1.6%) combined with a higher Mo content (compared with the other welds with the exception of SA 12) and its high oxygen level (474 ppm).

Toughness Evaluation

The variation in toughness of the welds reflects the differences in wire chemistry and flux formulation and their effects on microstructure and inclusions since strain and heat input effects are minimized and held constant (7). For a defect assessment, the minimum of three CTOD test values is used. It can be shown (7) that the probability of the minimum value of three tests is at or just above the mean value of the true distribution is 12.5%. This also represents the risk that the true mean is lower than the minimum of three tests. If the minimum of more then three test is used (e.g., 4, 5, 6, etc.) then the risk, that the true mean is lower than the minimum value, is reduced. For more than three test values a value higher than the minimum value may be used while maintaining the same or lower risk as the minimum of three tests. This probability can be calculated using a binomial distribution. It can be shown that six test results are required before the minimum value can be ignored and the second lowest value used while still maintaining a risk equal to or lower than that associated with the minimum of three tests. Hence, for four or five tests, the minimum value must be used, however, the level of risk is reduced.

Failure Mechanisms

Ductile failure, which occurs in the upper shelf regions of Charpy-temperature curves, is controlled by microstructure and the number of

non-metallic inclusions. Failure occurs by void formation and growth at oxy-sulphide inclusions. The volume fraction of these inclusions is directly related to the O + S content of the weld metal (Table 7). Ten of the 12 welds have O + S levels between 0.028% and .047% with SA 12 the lowest at 0.019% and SA 10 the highest at 0.058%. Examination of the Charpy transition curves of Fig. 2 to 5 and the O + S levels in Table 7 indicate that further testing at temperatures above 20°C is necessary to establish the upper shelf behaviour properly.

Failure in the lower shelf region of the Charpy transition curves and in the CTOD specimens (except for the δ_m values) occurred as a result of cleavage. CTOD fracture surfaces were examined in the scanning electron microscope (SEM). As in the previous study on SMAW (7) welds and the earlier study by Gianetto and Braid (23), failure was shown to occur by cleavage initiating at non-metallic, oxy-sulphide inclusions 1 μm diam or larger as shown in Fig. 12. Initiation occurred in as-deposited weld metal in grain-boundary ferrite or ferrite with second phase microstructures, this is in agreement with the observations of Tweed and Knott (24).

All fractures in the CTOD tests originated in the centre 1/3 portion of the testpiece. All welds had 80% or more as-deposited structure through the full plate thickness and, except for weld SA 8, had 68% or more as-deposited structure in the centre 1/3 portion. Weld SA 8 had 49% as-deposited in the centre 1/3 portion. Reheated weld-metal microstructures generally have higher fracture toughness (24,25), however, the large proportions of as-deposited structures in the 12 welds tested dominate the toughness behaviour.

Previous work evaluating SMAW consumables (7) and studies by Gianetto and Braid (23) and Judson and McKeown (1) have shown the importance of the size distribution of non-metallic inclusions in determining low temperature fracture toughness. These studies have shown improved toughness when the number of large inclusions (>1 μm diam) which act as cleavage crack initiation sites are reduced . Shehata et al. (26) have shown results for two SMA welds with similar strengths, microstructures and oxygen + sulphur levels. One weld had a significantly higher number of large inclusions compared with the other weld and consequently had lower CTOD values. This was a result of differences in electrode coating formulations. When the O + S levels are different an additional factor is observed; the higher the inclusion content

(O + S level) the higher the probability of obtaining a greater number of large inclusions. Hence, for improved toughness the O + S levels and corresponding volume fraction of non-metallic inclusions should be kept low as well as having a consumable formulation which has a tendency towards small, <1 μm diam, inclusions.

Charpy and CTOD Toughness

The differences between the Charpy test and the CTOD test for weld metals has been highlighted by Gianetto and Braid (23). Both welds studied had similar microstructures and strength. The SMA weld had a high volume fraction of inclusions and a greater number of large inclusions >1 μm diam compared with the SA weld in the study. Both welds had similar Charpy results in the lower shelf and transition regions but the submerged-arc weld had superior fracture toughness at -30°C and -10°C compared with the SMA weld. The difference can be explained using the model of Ritchie et al. (27) as shown in Fig. 13. Since the average spacing of large, >1 μm diam, inclusions was greater for the SA weld compared with the SMA weld then the distance, ℓ, from the crack tip to the initiating inclusion is larger for the SA weld than for the SMA weld. Hence, for the SA weld, a larger CTOD is required for the stress, σ_{yy}, to become greater than the fracture stress, σ_F, at the initiating inclusion. However, the stress ahead of a round notch, as in a Charpy specimen, does not increase as rapidly as for a sharp crack and when the stress, σ_{yy}, ahead of the notch reaches the fracture stress, σ_F, initiation sites are available for both welds. Although initiation of cleavage occurs by the same mechanism in both types of specimens it is the fracture stress of the welds which controls the lower shelf and transition region Charpy energies. The fracture stress is controlled primarily by microstructure and weld metal chemistry. Both Charpy and CTOD (or other fracture mechanics tests) are thus necessary to properly evaluate the toughness of weld metals.

The Charpy results for the C-Mn welds, shown in Fig. 2, are similar to each other. This can be related directly to the similar chemistries (Table 4) and corresponding microstructures (Table 10). The four welds in this group (SA 1, 4, 9 and 11) have chemistries of 0.1%C, 1.4% Mn, 0.3% Si, 0.01% Ti and oxygen contents of approximately 220 ppm. This is very close to the optimal chemistry discussed in Ref. (7) for SMA C-Mn weld metals. However, the Charpy toughnesses of the SA welds are, in general, lower than for

their SMAW counterparts (7). This is attributable to the higher acicular ferrite content of the SMA welds due to a lower heat input (2 kJ/mm-SMAW vs 2.8 kJ/mm-SAW).

The CTOD values measured for the C-Mn welds are considerably better than those measured for the C-Mn SMA welds in the previous study. All values are above 0.08 mm. The CTOD values, given in Table 8 also show a considerable increase in scatter at -10°C. Values above 0.2 mm generally showed ductile tearing before failure with the highest values at -10°C, for welds SA 1, 4 and 11, giving maximum load values. Welds SA 1, 4 and 11 gave similar CTOD behaviour while SA 9 showed poor fracture toughness as a result of the higher oxygen content (365 ppm) and probable higher number of large inclusions. This weld also had the lowest amount of acicular ferrite (55%) in the group.

The Charpy results of the three C-Mn-1 Ni welds shown in Fig. 3 are similar to those for the C-Mn welds except for weld SA 7 which exhibited a higher toughness. The 35 J temperatures and lower shelf energy levels are slightly higher than the C-Mn welds reflecting slight increase in acicular ferrite content to between 62% and 67% and the improved cleavage resistance of ferrite with nickel addition. The improved toughness of weld SA 7 compared with SA 2 and 5 is attributable in part to the slightly lower Mn level (1.28% compared with 1.4%) resulting in a small decrease in strength (~40 MPa for yield and ultimate).

The CTOD results for the C-Mn-1 Ni welds generally show a slight improvement compared to the C-Mn welds, which was attributed to the small increase in acicular ferrite content.

Weld SA 6, a C-Mn-3 Ni weld, shows similar Charpy behaviour (Fig. 4) to the C-Mn-1 Ni welds. Like the C-Mn-1 Ni welds, SA 6 has 65% acicular ferrite but has a chemistry with reduced Mn (1.23% compared with 1.4% with the 1 Ni welds) to compensate for the increased Ni content. Weld SA 6 nominally should have 3% Ni but the analysis (Table 4) shows only 1.4%. Dilution would account for some of the difference but it is not known why the value is half of what it should be. Weld SA 8, nominally a 2% Ni weld (1.5 % deposit analysis), shows poor Charpy toughness resulting from a microstructure with a low amount (40%) of acicular ferrite. The chemistry, including oxygen level, is similar to SA 6 (Table 4) and it is thought that there may be fewer inclusions of the correct type for nucleating acicular ferrite than present in the other welds.

Weld SA 6 has similar CTOD results compared with the C-Mn-1 Ni welds. Weld SA 8, however, had three CTOD values below 0.08 mm at -30°C and all values were below 0.2 mm. This is attributable, as in the Charpy results, to the low amount of acicular ferrite and also indicates a possible problem with large inclusions.

The two C-Mn-Ti-B welds, SA 3 and SA 10, and the C-Mn-Mo weld, SA 12, showed the best Charpy toughness of all the welds. This is attributed to their high amount of acicular ferrite microstructure (76% to 84%). Weld SA 10 has lower toughness compared with SA 3 and SA 12 but is still higher than the C-Mn-1 Ni welds tested. This weld also had the highest strength of all welds tested (50-60 MPa higher yield stress than SA 3 and SA 12). The lower toughness results from the higher strength (due to high Mn level ~1.6%) and the substantially higher oxygen content (474 ppm). The Ti-B welds achieve their high proportions of acicular ferrite from the boron addition while the C-Mn-Mo weld achieves its high acicular ferrite content by having a near optimum chemistry according to Ito and Nakanishi (4). This will be discussed further in the section on microstructure.

The CTOD results for welds SA 3 and SA 12 are also the highest of all the welds, again as a result of low inclusion level and high proportions of acicular ferrite. Weld SA 10, despite having 78% acicular ferrite, showed poor CTOD values as a result of having the highest oxygen content (474 ppm) of all the welds. This results in an increased probability of having a greater number of large inclusions.

Microstructure

The microstructure of all 12 welds are compared by Charpy toughness in Table 11. The welds in this table are listed in order of decreasing toughness, based on the 35 J temperature given in Table 7. The trend shown in Table 11 is for increasing toughness with increasing amounts of acicular ferrite. Acicular ferrite has been shown to act as a barrier to cleavage crack propagation (24,28) due to the small grain size of this structure causing cracks to stop and reinitiate at high angle grain boundaries. Cleavage cracks were shown to preferentially follow the much larger grain boundary ferrite veins.

The development of acicular ferrite microstructures depends upon the correct combination of weld metal chemistry, cooling rate and size, size-distribution, shape and composition of oxide inclusions. Fluxes serve to protect the molten weld pool from the atmosphere while elements added to the flux react with the molten metal to remove oxygen. Highly basic fluxes have been shown to produce the lowest oxygen levels and corresponding low level of inclusions in weld metals. Oxide inclusions affect the formation of acicular ferrite in two ways. First, in high oxygen welds (∿550 ppm and up) the inclusions act to pin austenite grain boundaries (29) producing small austenite grains. The resulting larger grain boundary surface area provides an increased number of grain boundary ferrite nucleation sites (5,14,16,18,21,29). Transformation temperatures are higher (15,21) and the formation of grain boundary ferrite and ferrite with second phase structures are favored. Lower oxygen levels (∿200 ppm) result in larger austenite grains and lower amounts of grain boundary ferrite with an associated decrease in transformation temperature owing to increased intragranular nucleated ferrite. The second effect of inclusions is on the actual nucleation of acicular ferrite. Oxide inclusions have been shown to act as nucleation sites for acicular ferrite (14,17,19-21). Not all the oxide particles produced are suitable nucleants. Suitable nucleants are generally in the size range 0.2 to 0.75 μm diameter (17,19,21). The influence of shape of inclusions has been studied (16-18) with no clear picture yet to emerge. Nucleating oxides have been shown to be made up of complex combinations of Mn, Si, Ti and Al as well as traces of other elements (13,19,20). It is unclear at this time as to the exact mechanism by which inclusions nucleate acicular ferrite; by providing sites with favorable surface energy, crystallographic orientation, shape or a combination of these factors.

Weld metal chemistry is another important factor in developing favorable acicular ferrite microstructures. Some of the major alloy additions, such as Mn, Si and Ti, are also oxide formers and hence chemistry and inclusion formation are intrinsically interconnected. Apart from forming acicular ferrite, alloy additions, such as nickel are made to refine the acicular ferrite and to increase the cleavage resistance of ferrite. Silicon, used as a deoxidizer and hardenability agent, also is necessary for arc transfer characteristics (particularly in out of position welding) but in too high a quantity

decreases toughness by decreasing the cleavage resistance of ferrite and promoting bainitic microstructures (30). A balance of elements is required to optimize toughness and this will vary from one alloy system to another.

The C-Mn welds tested (SA 1, 4, 9 and 11) had similar compositions of approximately 0.11% C, 1.45% Mn, 0.3% Si and 0.01% Ti. This is close to the suggested composition for C-Mn submerged arc welds by Tuliani et al. (30): 0.1% C, 1.2-1.4% Mn and 0.18-0.20% Si. The C-Mn welds in the previous SMA weld tests (7) had 0.08%C, 1.4% Mn, 0.35% Si and 0.02% Ti, giving 75% acicular ferrite compared to the 60% for the submerged arc welds.

The C-Mn-1 Ni welds (SA 2, 5 and 7) showed a slight increase in the amount of acicular ferrite, to ~65%, with the same composition as the C-Mn welds plus 1% Ni (0.70% deposit). The addition of nickel above 1% is accompanied by a decrease in Mn content (1,31). Welds SA 6 and 8, both with 1.5% Ni (deposit) had lower Mn levels at 1.2-1.25%, similar to the SMA welds studied previously (7). Like the SMA 2 1/2% and 3 1/2 Ni welds (7), SA 6 and 8 had lower amounts of acicular ferrite (65% and 40% respectively). However, unlike the SMA welds the Charpy toughness did not improve relative to the C-Mn welds.

The addition of Ti and B to C-Mn weld metals has been shown to improve toughness by increasing acicular ferrite content (3,10,11,12,13). As discussed earlier, Ti is required in the inclusions to nucleate acicular ferrite. The role of boron is somewhat more complex. However, most researchers agree that boron segregates to austenite grain boundaries reducing the grain boundary energy and thus suppressing the formation of grain boundary ferrite (12). The optimum Ti and B levels are given by Tsuboi and Terashima (12) as 0.02-0.03% Ti and 0.003-0.005% B although this may vary somewhat depending on the nitrogen level (and hence welding process). Kohno et al. (11) give optimum Ti as 0.015% to 0.025% with B levels at equivalent wt % as the weld metal nitrogen content. For welds SA 3 and 10 the Ti and B contents are within these optimum ranges.

Welds SA 3 and SA 10 also contain some Mo, the specific addition in SA 12 which had the highest amount of acicular ferrite (84%). Pacey et al. (32) showed an increase in amount of acicular ferrite (75% to 85%) with increasing Mo in the range 0.25% to 0.48% while Ito and Nakanishi (4) gave the optimum Mo content to be about 0.25%. Welds SA 10 and 12 have 0.25% and 0.28% Mo respectively, and have the highest amounts of acicular ferrite (83% and 84% respectively).

CONCLUSIONS

Ten of the twelve submerged-arc welds tested would meet a 0.08 mm CTOD requirement at -30°C while two of the welds would meet a 0.2 mm CTOD requirement at -30°C. However, only three welds would meet a Charpy requirement of 35 J at 20°C below a design temperature of -30°C (i.e., -50°C test temperature). The welds showing the best toughness were associated with microstructures consisting of 75% or more acicular ferrite.

As in the previous evaluation of shielded-metal-arc welds (7) low temperature fracture occurred by cleavage initiation from large, >1 μm diam, inclusions primarily in grain boundary ferrite. Poor toughness was associated with welds with high oxygen levels and hence high inclusion volume fractions. The weld with the highest oxygen content, weld SA 10 (474 ppm), still displayed good toughness relative to the C-Mn welds owing to the high proportion of acicular ferrite microstructure.

Improved toughness was associated with high proportions of fine-grain acicular ferrite microstructures. Weld metal chemistries of 0.1% C, 1.45% Mn, 0.3% Si and 0.01% Ti for the C-Mn welds gave an acicular ferrite content of approximately 60%. The levels of C, Mn, Si and Ti are close to those of other researchers that gave optimum toughness. Additions of up to 1% Ni were shown to increase toughness slightly due to a small increase in acicular ferrite to approximately 65%. Increasing nickel additions above 1% resulted in a small decrease in toughness due to a decrease in the amount of acicular ferrite despite a concurrent decrease in Mn content. The similar alloy system in SMA welds shows improved toughness at 2 1/2% and 3 1/2% Ni additions. It is suspected that a smaller austenite grain size and an insufficient number of preferred nucleation sites for acicular ferrite are responsible.

The highest proportions of acicular ferrite and best toughness were associated with additions of Ti, B and/or Mo to the C-Mn weld chemistry described above. Additions of 0.25% Mo, 0.01-0.03% Ti and 0.001 to 0.003% B produced microstructures with 76% to 84% acicular ferrite. The toughness of weld SA 10 could be improved by reducing the oxygen level (inclusion level) and lowering the Mn from 1.6 to 1.4%.

FUTURE WORK

The toughness of submerged-arc welds is, in general, better than that of shielded-metal-arc welds reflecting the more advanced stage of development of the SA process in this respect. However, further work is required in the following areas:

1. An understanding of the mechanism of nucleation of acicular ferrite structures is required to enable the correct choice of alloy additions and welding flux constituents to maximize the amount of this structure in a weld deposit. This would include the effects of various elements in the non-metallic inclusions which act as nucleation sites.
2. The mechanism by which boron, titanium and nitrogen interact to inhibit grain boundary ferrite and promote acicular ferrite still needs to be determined.
3. Further work is required to optimize weld metals with 2% or more nickel additions if the known improvements in cleavage resistance of ferrite are to be exploited.

ACKNOWLEDGEMENTS

The authors would like to thank R.F. Orr and D.E. Dolan for technical assistance during the course of this work.

REFERENCES

1. Judson, P. and McKeown, D. Proc. 2nd Int. Conf. Offshore Welded Structures, Weld. Inst., London, 1982. Paper 3.

2. Taylor, L.G. and Farrar, R.A., Weld. and Met. Fab., Vol. 43, No. 4, 1985. pp 305-310.

3. Garland, J.G. and Kirkwood, P.R., Met. Const., Vol. 7, No.5 & 6, 1975. pp 275-283 and 320-330.

4. Ito, Y. and Nakanishi, M., Sumitomo Search, No. 15, May 1976. pp 42-62.

5. Cochrane, R.C. and Kirkwood, P.R., Proc. Int. Conf. Trends in Steels and Consumables for Welding, Weld. Inst., London, 1978. pp 103-121.

6. Garland, J.G. and Kirkwood, P.R., Weld. and Met. Fab., Vol. 44, No. 3, 1976. pp 217-224.

7. Braid, J.E.M. and Gianetto, J.A., Division Report PMRL 86-99(TR).

8. Pargeter, R.J. and Dolby, R.E., IIW Doc. No. IXJ-102-85, 1985.

9. Evans, G.M., Weld. J., Vol. 59, No. 3, 1980. pp 67s-75s.

10. Still, J.R. and Rogerson, J.H., Met. Const., Vol. 10, No. 7, 1978. pp 339-342.

11. Kohno, R., Takami, T., Mori, N. and Nagano, K., Weld. J., Vol. 61, No. 12, 1982. pp 373s-380s.

12. Tsuboi, J. and Terashima, H., Welding in the World, Vol. 12, No. 11/12, 1983. pp 304-316.

13. Ohkita, S., Homma, H., Tsushima, S. and Mori, N., Australian Welding, Vol. 29, No. 3, 1984. pp 29-36.

14. Abson, D.J., Dolby, R.E. and Hart, P.H.M., Int. Conf. Trends in Steels and Consumables for Welding, Weld. Inst., London, 1978. Paper 25.

15. Harrison, P.L. and Farrar, R.A., J. Mat. Sci., Vol. 16, 1981. pp 2218-2226.

16. Cochrane, R.C. and Keville, B.R., Proc. Conf. Steel for Linepipe and Pipeline Fittings, Weld. Inst., London, 1981. pp 51-60.

17. Ricks, R.A., Howell, P.R. and Barritte, G.S., J. Mat. Sci., Vol. 17, 1982. pp 732-740.

18. Keville, B.R., Weld. J., Vol. 62, No. 9, 1983. pp 253s-260s.

19. Kayali, E.S., Corbett, J.M and Kerr, H.W., J. Mat. Sci. Lett., Vol. 2, 1983. pp 123-128.

20. Bhatti, A.R., Saggese, M.E., Hawkins, D.N., Whiteman, J.A. and Golding, M.S., Weld. J., Vol. 63, No. 7, 1984. pp 224s-230s.

21. Liu, S. and Olson, D.L., Weld J., Vol. 65, No. 6, 1986. pp 139s-149s.

22. Pisarski, H.G. and Harrison, J.D., "Welding for Challenging Environments"; Proc. Int. Conf., Toronto; Pergamon Press, Toronto, 1986. pp 131-144.

23. Gianetto, J.A. and Braid, J.E.M., Division Report PMRL 85-71(TR).

24. Tweed, J.H and Knott, J.F., Met. Sci., Vol. 17, No. 2, 1983. pp 45-54.

25. Stout, R.D. McLaughlin, P.F. and Strunk, S.S., Weld. J., Vol. 48, No. 4, 1969. pp 155s-160s.

26. Shehata, M., Chandel, R.S., Braid, J.E.M. and McGrath, J.T., Micro. Sci., Vo. 14, 1987. pp 65-76.

27. Ritchie, R.O., Francis, B. and Server, W.L., Met. Trans., Vol. 7A, No. 6, 1976. pp 831-838.

28. McRobie, D.E. and Knott, J.F., Met. Sci. and Techn., Vol. 1, 1985. pp 357-365.

29. Haroun, N.A., J. Mat. Sci., Vol. 15, 1980. pp 2816-2822.

30. Tuliani, S.S., Ceram, A.I. and Farrar, R.A., Weld, and Met. Fab., Vol. 43, No. 7, 1975. pp 553-558.

31. Taylor, D.S. and Evans, G.M., Met. Const., Vol. 15, No. 8, 1983. pp 438-443.

32. Pacey, A.J., Kayali, S. and Kerr, H.W., Can. Met. Q., Vol. 21, No. 3, 1982. pp 309-318.

Table 1 - Chemical composition of 350 WT base material

Base material	Element wt %										
	C	Mn	Si	S	P	Al	Cu	Ni	Cr	V	Nb
350 WT	0.15	1.44	0.24	0.005	0.015	0.015	0.015	0.225	0.040	0.060	0.020

Table 2 - Submerged-arc welding wire composition

Weld Identification	Element (wt%)												
	C	Mn	Si	S	P	Ni	Mo	Cr	Al	V	Nb	Ti	B
C-Mn													
SA 1	0.11	1.70	0.280	0.016	0.012	0.034	0.005	0.060	0.093	0.001	0.012	0.001	<0.0005
SA 4	0.12	1.80	0.250	0.014	0.012	0.038	0.014	0.048	0.120	0.001	0.014	0.001	<0.0005
SA 9	0.13	1.90	0.076	0.012	0.008	0.063	0.025	0.037	0.100	<0.001	0.014	0.032	<0.0005
SA 11	0.13	1.70	0.260	0.009	0.009	0.042	0.040	0.061	0.088	<0.001	0.021	0.002	0.0011
C-Mn- 1Ni													
SA 2	0.11	1.60	0.120	0.016	0.017	1.30	0.006	0.045	0.061	0.002	0.012	<0.001	<0.0005
SA 5	0.12	1.60	0.220	0.011	0.008	1.20	0.033	0.044	0.120	0.003	0.017	0.002	<0.0005
SA 7	0.07	1.00	0.620	0.006	0.013	1.00	0.037	0.028	0.080	0.006	0.016	0.001	<0.0005
C-Mn- 2-3Ni													
SA 6	0.07	1.10	0.220	0.011	0.005	2.60	0.065	0.048	0.130	0.003	0.018	<0.001	<0.0005
SA 8	0.12	0.94	0.032	0.009	0.010	2.50	0.090	0.038	0.062	0.010	0.025	0.005	<0.0005
C-Mn-Ti-B													
SA 3	0.07	1.20	0.037	0.008	0.009	0.063	0.250	0.110	0.094	0.003	0.011	0.045	0.0040
SA 10	0.11	1.10	0.440	0.013	0.005	0.029	0.550	0.047	0.130	0.016	0.021	0.170	<0.0005
C-Mn-Mo													
SA 12	0.10	1.50	0.240	0.015	0.007	0.038	0.580	0.050	0.068	0.001	0.021	<0.001	0.0007

Table 3 - Typical submerged-arc welding parameters

Pass No.	Current DCEP amps	Voltage volts	Wire feed speed mm/s	Travel speed mm/s	Electrode extension mm
Side 1 1-2	∿600	32	21	6.8	32
Side 2 3	∿600	32	21	6.8	32

Note: i) Maximum interpass temperature = 150°C

ii) Welds SA 9, SA 10, SA 11 and SA 12 required three passes on side 1

Table 4 - Chemical composition of submerged-arc-weld metals

Weld No.	Element wt %														ppm	
	C	Mn	Si	S	P	Ni	Cr	Mo	Cu	Al	V	Nb	Ti	B	N	O
C-Mn																
SA 1	0.110	1.47	0.300	0.010	0.015	0.150	0.045	<0.005	0.060	0.021	0.035	0.015	0.010	0.0003	94	218
SA 4	0.120	1.50	0.290	0.010	0.016	0.145	0.050	<0.005	0.105	0.020	0.035	0.015	0.010	0.0006	86	221
SA 9	0.106	1.33	0.280	0.010	0.017	0.150	0.035	<0.005	0.085	0.010	0.030	0.015	0.015	0.0017	88	365
SA 11	0.105	1.48	0.300	0.008	0.017	0.130	0.045	<0.005	0.070	0.015	0.030	0.015	0.010	0.0005	79	204
C-Mn-1 Ni																
SA 2	0.100	1.41	0.285	0.010	0.016	0.640	0.040	<0.005	0.065	0.018	0.035	0.015	0.010	0.0003	74	263
SA 5	0.110	1.43	0.270	0.008	0.015	0.700	0.045	<0.005	0.060	0.020	0.035	0.017	0.010	0.0005	95	206
SA 7	0.105	1.28	0.380	0.008	0.015	0.550	0.054	<0.005	0.040	0.015	0.035	0.017	0.010	0.0003	64	248
C-Mn-2-3 Ni																
SA 6	0.103	1.23	0.263	0.010	0.013	1.40	0.045	0.010	0.085	0.020	0.035	0.017	0.010	0.0005	88	273
SA 8	0.115	1.25	0.225	0.008	0.014	1.50	0.036	<0.005	0.018	0.025	0.035	0.017	0.010	0.0003	67	205
Ti-B																
SA 3	0.100	1.25	0.205	0.008	0.015	0.155	0.065	0.110	0.065	0.018	0.035	0.014	0.010	0.0009	88	276
SA 10	0.096	1.60	0.360	0.011	0.015	0.140	0.035	0.250	0.050	0.010	0.035	0.017	0.030	0.0034	85	474
C-Mn-Mo																
SA 12	0.102	1.41	0.285	0.010	0.017	0.130	0.040	0.280	0.160	0.015	0.030	0.015	0.005	0.0005	95	182

Table 5 - Carbon equivalents of submerged-arc welds

Weld No.	C.E. IIW	Pcm	CEN
SA 1	0.38	0.21	0.31
SA 4	0.40	0.23	0.35
SA 9	0.35	0.21	0.29
SA 11	0.38	0.21	0.30
SA 2	0.39	0.22	0.30
SA 5	0.41	0.24	0.33
SA 7	0.37	0.22	0.29
SA 6	0.42	0.26	0.31
SA 8	0.44	0.27	0.34
SA 3	0.36	0.20	0.28
SA 10	0.44	0.24	0.34
SA 12	0.42	0.22	0.33

Table 6 - Tensile properties of submerged-arc-weld metals

Weld No.	Yield Strength MPa	Ultimate Strength MPa	Elongation %	Reduction of area %
C-Mn				
SA 1	530	638	27	66
SA 4	527	653	26	65
SA 9	530	626	28	67
SA 11	501	625	27	68
C-Mn-1 Ni				
SA 2	542	649	27	67
SA 5	546	673	27	65
SA 7	500	628	28	71
C-Mn-2-3 Ni				
SA 6	559	665	27	64
SA 8	504	639	21	64
C-Mn-Ti-B				
SA 3	530	631	25	68
SA 10	599	697	24	67
C-Mn-Mo				
SA 12	541	687	27	68

Table 7 - 35 J transition temperatures

Weld	35 J T.T. °C	O ppm	O + S wt %
SA 1	-26	218	0.032
SA 4	-34	221	0.032
SA 9	-33	365	0.047
SA 11	-32	204	0.028
SA 2	-40	263	0.036
SA 5	-40	206	0.028
SA 7	-47	248	0.033
SA 6	-38	273	0.037
SA 8	-13	205	0.029
SA 3	<-60	276	0.036
SA 10	-58	474	0.058
SA 12	<-60	182	0.019

Table 8 - CTOD properties of submerged-arc-weld metals

Test temp.	C-Mn				C-Mn-1 Ni			C-Mn-2-3 Ni		C-Mn-Ti-B		C-Mn-Mo
(°C)	SA 1	SA 4	SA 9	SA 11	SA 2	SA 5	SA 7	SA 6	SA 8	SA 3	SA 10	SA 12
-30°C	0.127(u)	0.089(u)	0.117(u)	0.269(u)	0.081(u)	0.135(u)	0.224(u)	0.495(m)	0.023(c)	0.643(u)	0.086(u)	0.460(u)
	0.135(u)	0.218(u)	0.099(u)	0.128(u)	0.231(u)	0.127(u)	0.140(u)	0.147(u)	0.079(u)	0.218(u)	0.180(u)	0.538(u)
	0.206(u)	0.254(u)	0.086(u)	0.178(u)	0.559(m)	0.282(u)	0.269(u)	0.300(u)	0.081(u)	0.600(m)	0.226(u)	0.635(m)
	0.206(u)	0.155(u)	0.104(u)	0.239(u)	0.592(m)	0.069(u)	0.218(u)	0.351(u)	0.147(u)	0.630(m)	0.122(u)	0.589(m)
	0.282(u)	0.173(u)	0.163(u)	0.084(u)	0.587(m)	0.264(u)	0.173(u)	0.140(u)	0.033(u)	0.572(m)	0.107(u)	0.229(u)
-10°C	0.150(u)	0.122(u)	0.102(u)	0.599(m)	0.536(m)	0.531(u)	0.140(u)	0.580(m)	0.135(u)	0.635(m)	0.208(m)	0.645(m)
	0.500(m)	0.516(m)	0.269(u)	0.419(u)	0.594(m)	0.218(u)	0.541(m)	0.633(m)	0.112(u)	0.569(m)	0.180(m)	0.538(u)
	0.236(u)	0.577(u)	0.254(u)	0.084(u)	0.645(m)	0.539(u)	0.615(m)	0.127(u)	0.165(u)	0.617(m)	0.150(u)	0.279(u)
	0.325(u)	0.366(u)	0.218(u)	-	0.478(m)	0.191(u)	0.295(m)	0.602(m)	0.191(u)	0.633(m)	0.178(m)	0.640(m)

Table 9 - Distribution of as-deposited (columnar) (A) and reheated (R) regions

Weld No.	Total plate thickness A	R	CVN location A	R	Central 1/3 location A	R
C-Mn						
SA 1	94	6	88	12	82	18
SA 4	92	8	84	16	76	24
SA 9	89	11	79	21	68	32
SA 11	94	6	88	12	83	17
C-Mn-1 Ni						
SA 2	91	9	82	18	72	28
SA 5	91	9	84	16	75	25
SA 7	93	7	86	14	78	22
C-Mn-2-3 Ni						
SA 6	93	7	88	12	80	20
SA 8	80	20	60	40	49	51
C-Mn-Ti-B						
SA 3	92	8	84	16	75	25
SA 10	92	8	83	17	75	25
C-Mn-Mo						
SA 12	93	7	85	15	78	22

Table 10 - Percentage of microstructural constituents in the as-deposited weld metal region

Weld No.	Percentage of constituents				
	AF	GF	FS(A)	FS(N)	PF
C-Mn					
SA 1	62	22	8	3	5
SA 4	60	22	7	6	5
SA 9	55	32	4	5	4
SA 11	61	23	6	5	5
C-Mn-1 Ni					
SA 2	62	25	4	3	6
SA 5	67	15	4	7	7
SA 7	67	19	4	4	6
C-Mn-2-3 Ni					
SA 6	65	20	7	4	4
SA 8	40	10	30	18	2
C-Mn-Ti-B					
SA 3	76	20	2	0	2
SA 10	83	9	2	3	3
C-Mn-Mo					
SA 12	84	9	3	2	2

AF = acicular ferrite

GF = grain boundary ferrite

FS( ) = ferrite with second phase (A) aligned (N) nonaligned

PF = polygonal ferrite

Table 11 - Comparison of Charpy toughness and microstructure

Weld*	% AF	% GF	O + S (wt %)
SA 12	84	9	0.019
SA 3	76	20	0.036
SA 10	83	9	0.058
SA 7	67	19	0.033
SA 2	62	25	0.036
SA 5	67	15	0.028
SA 6	65	20	0.037
SA 4	60	22	0.032
SA 9	55	32	0.047
SA 11	61	23	0.028
SA 1	62	22	0.032
SA 8	40	10	0.029

*Welds in order of decreasing toughness

AF = acicular ferrite

GF = grain boundary ferrite

O + S = oxygen + sulphur

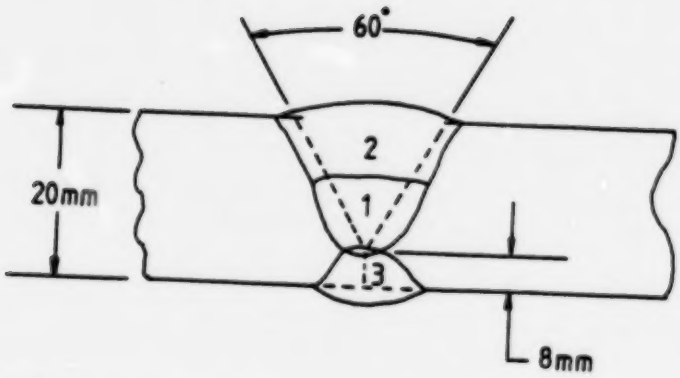

Fig. 1 Typical pass sequence for experimental welds. (neg. 15486).

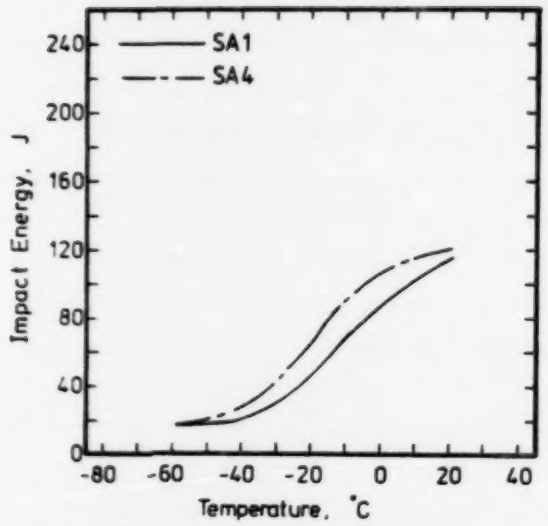

(a) (neg.15485)

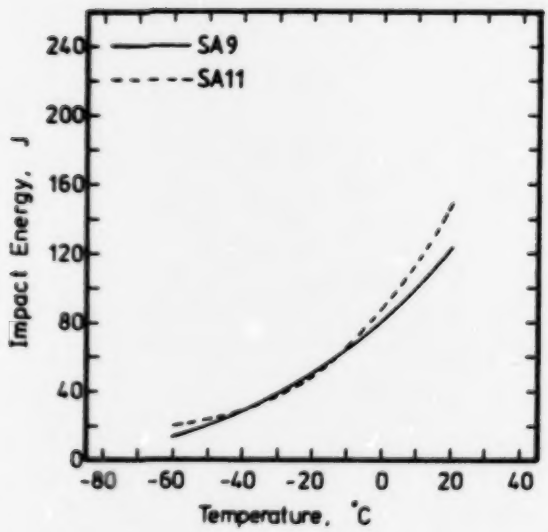

(b) (neg.15470)

Fig. 2 Charpy impact transition curves for C-Mn welds.

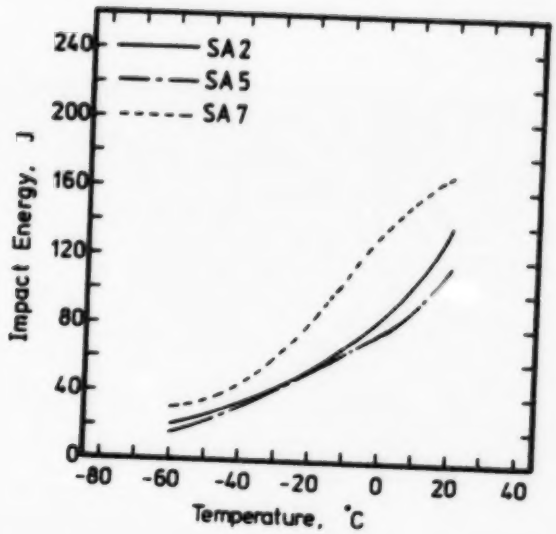

Fig. 3 Charpy impact transition curves for C-Mn-1% Ni welds. (neg.15469)

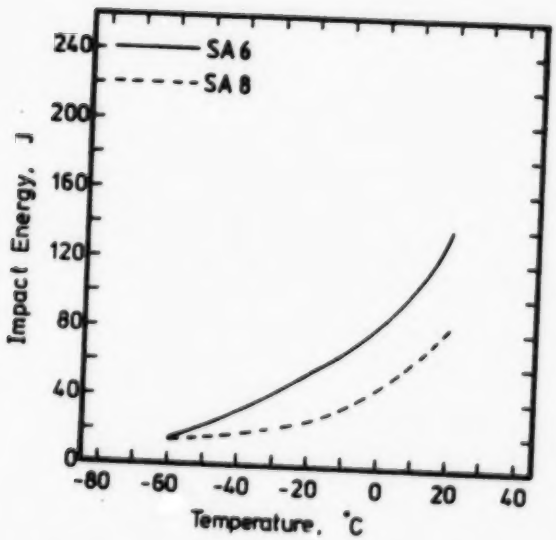

Fig. 4 Charpy impact transition curves for C-Mn-2-3% Ni welds. (neg.15472)

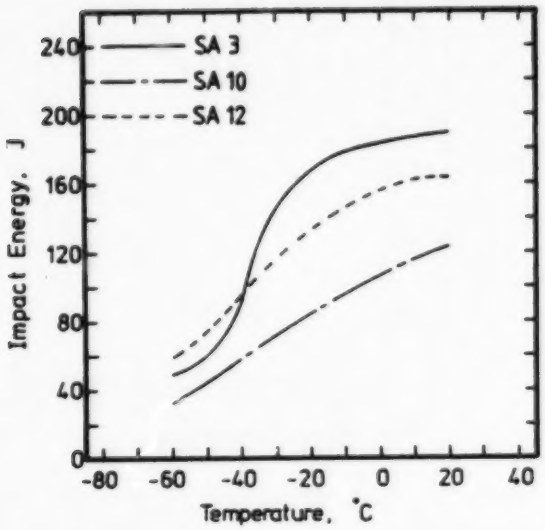

Fig. 5 Charpy impact transition curves for C-Mn-Ti-B and C-Mn-Mo welds. (neg.15471).

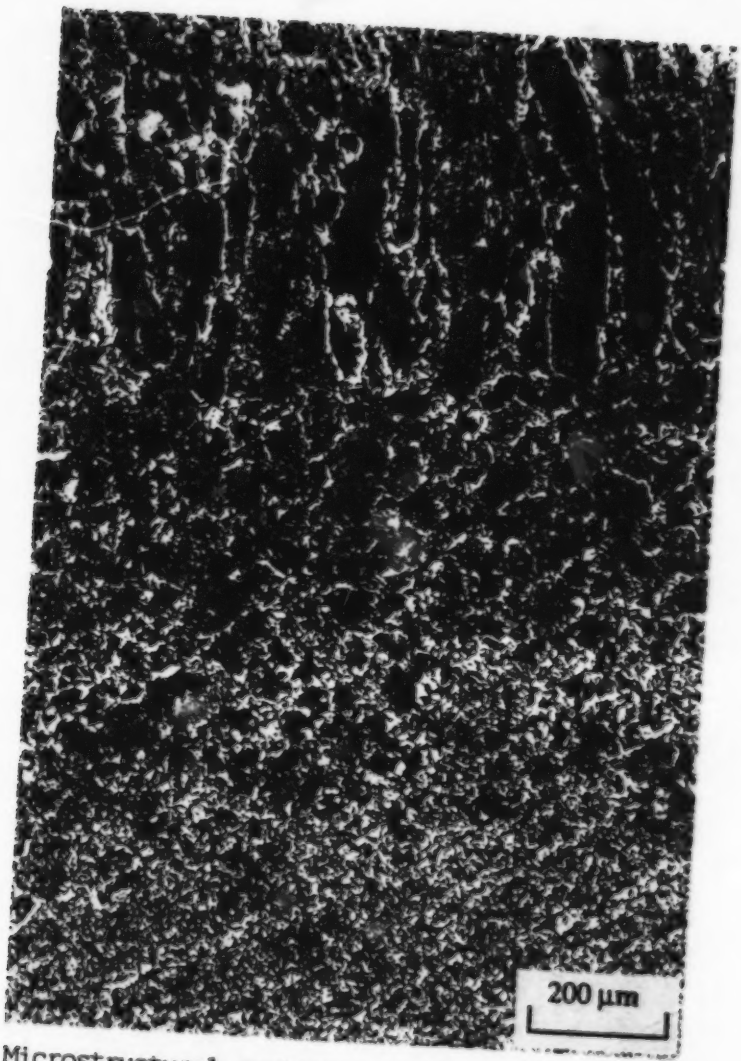

Fig. 6 Microstructural regions at weld centerline showing as-deposited (columnar), coarse and fine grain reheated structures. (neg.17524).

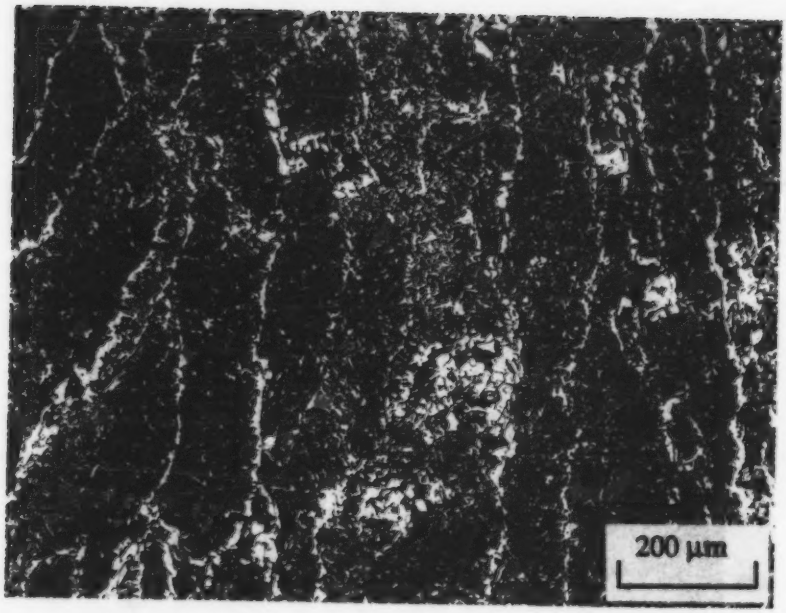

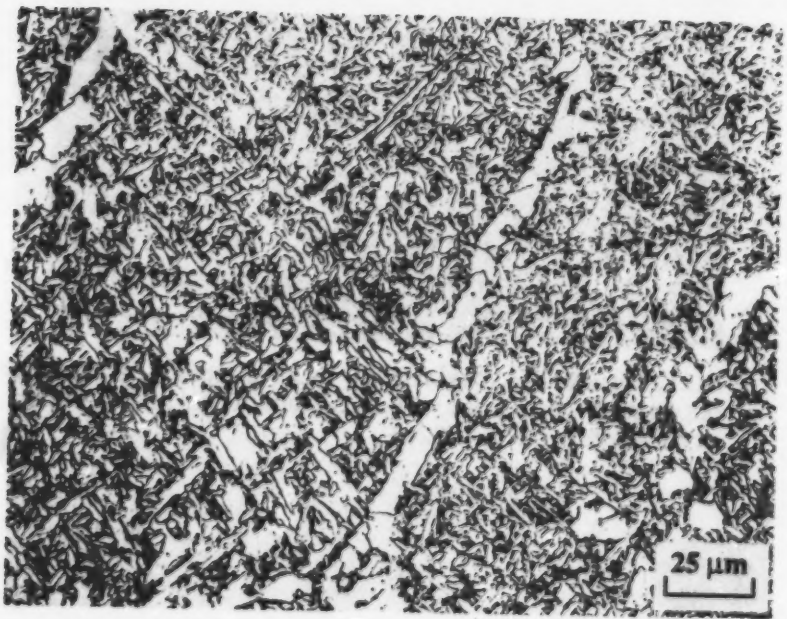

(a) Weld SA1 (neg.17525 and 17526)

Fig. 7 Cont'd

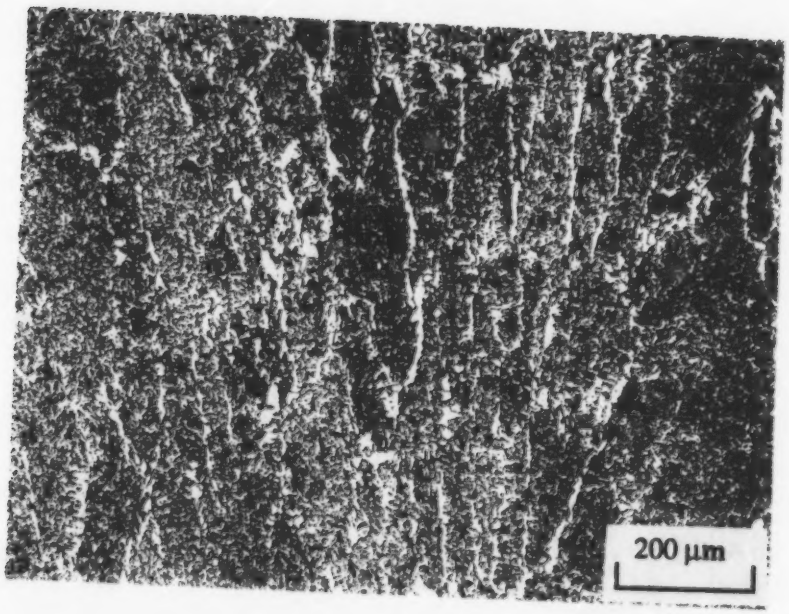

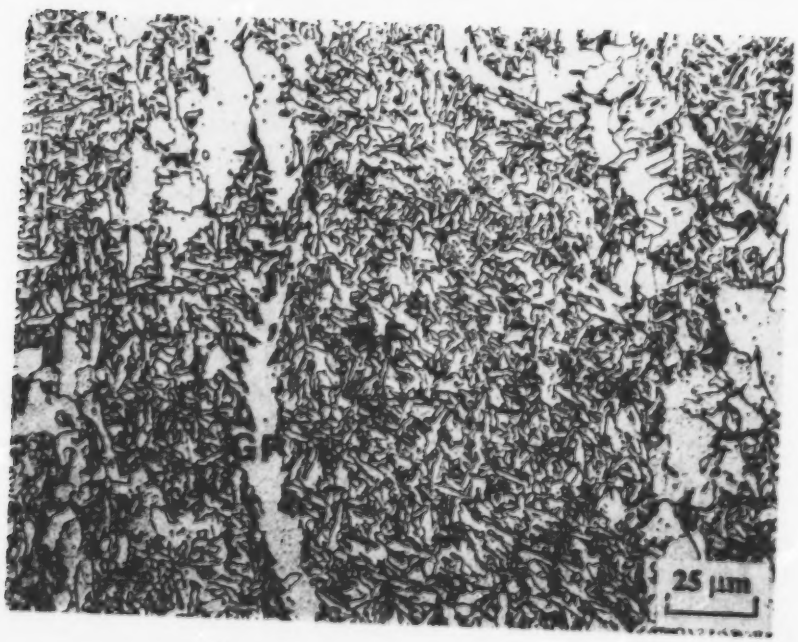

(b) Weld SA4 (neg.17527 and 17528)
Microconstituents; AF-Acicular Ferrite and GF-Grain Boundary Ferrite

Fig. 7 Cont'd

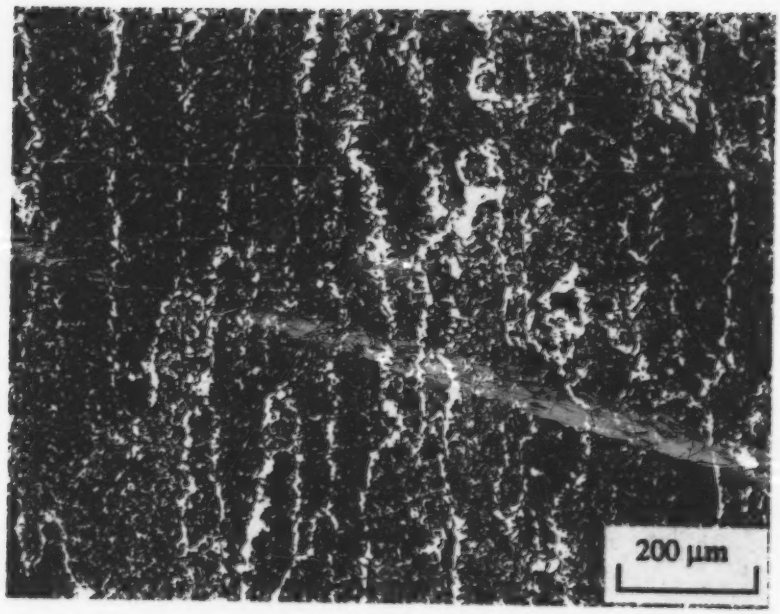

(c) Weld SA9 (neg.17529 and 17530)

Fig. 7 Cont'd

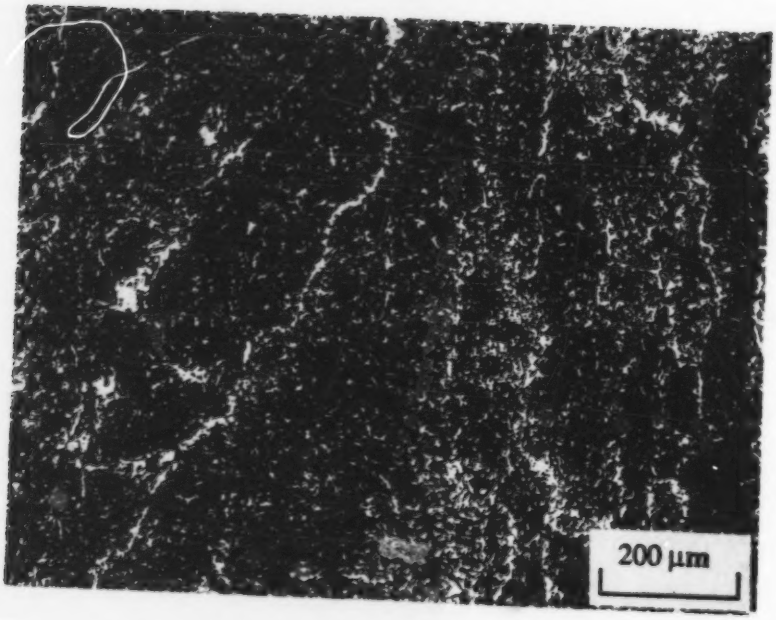

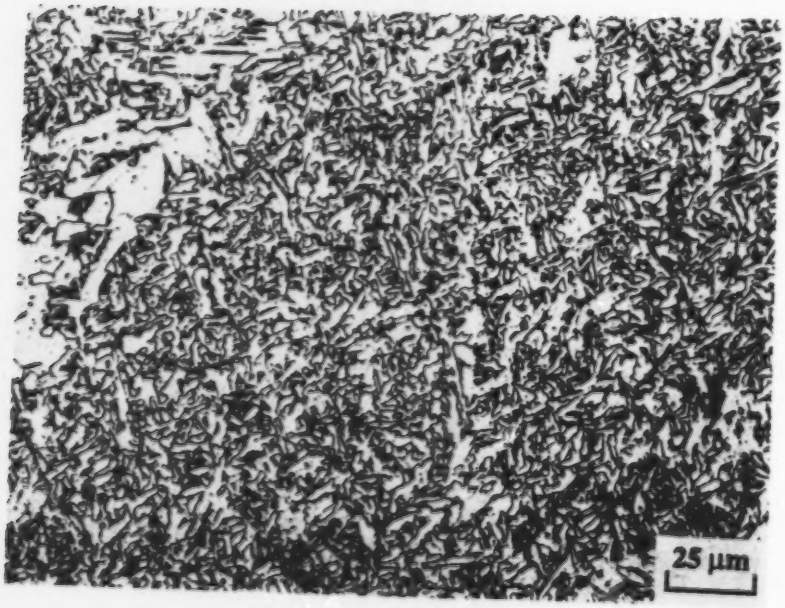

(a) Weld SA11 (neg.17531 and 17532)

Fig. 7 Microstructure of C-Mn as-deposited weld metals.

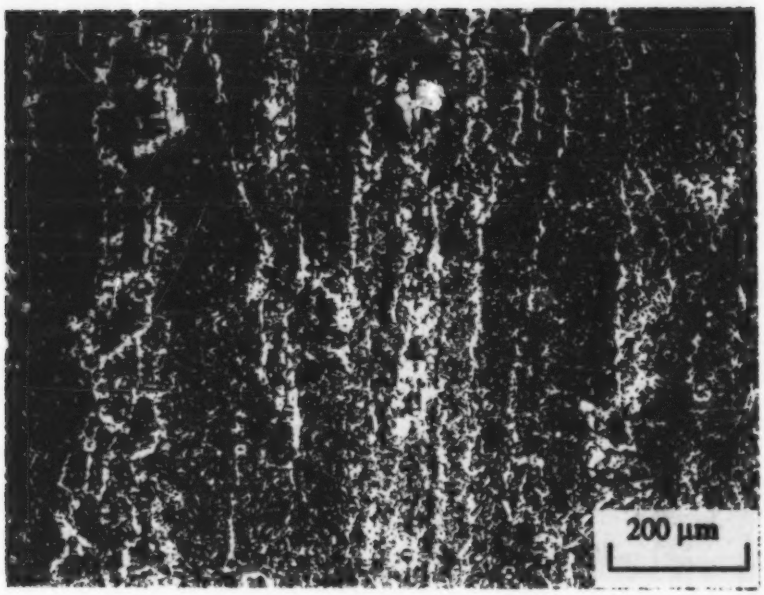

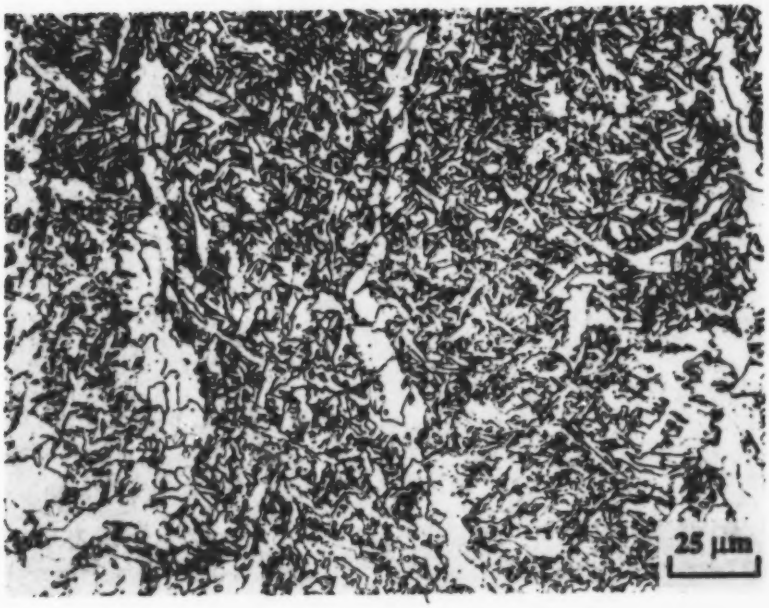

(a) Weld SA2 (neg.17533 and 17534)

Fig. 8 Cont'd

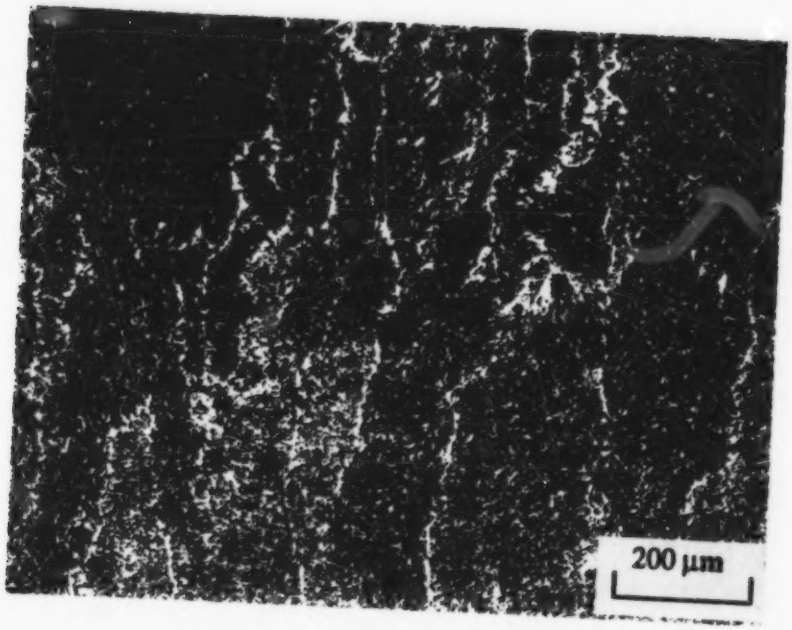

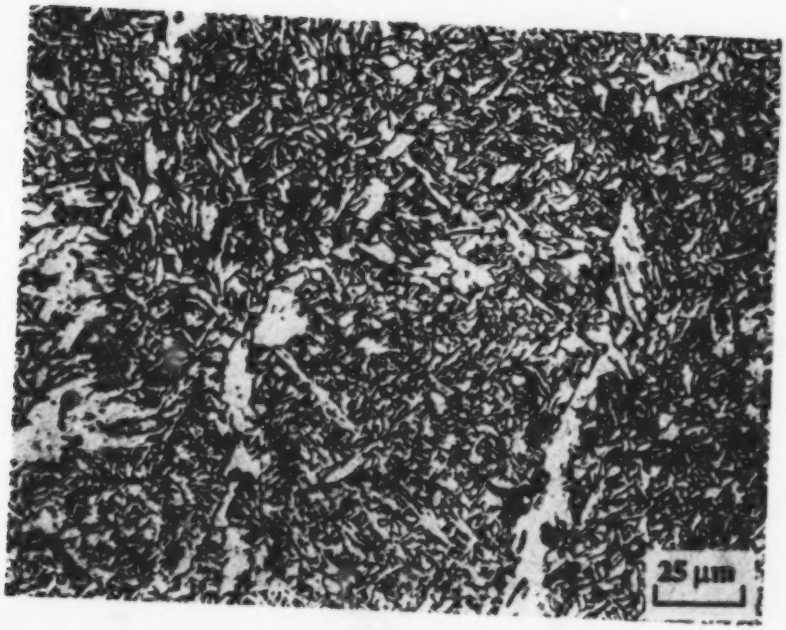

(b) Weld SA5 (neg.17535 and 17536)

Fig. 8 Cont'd

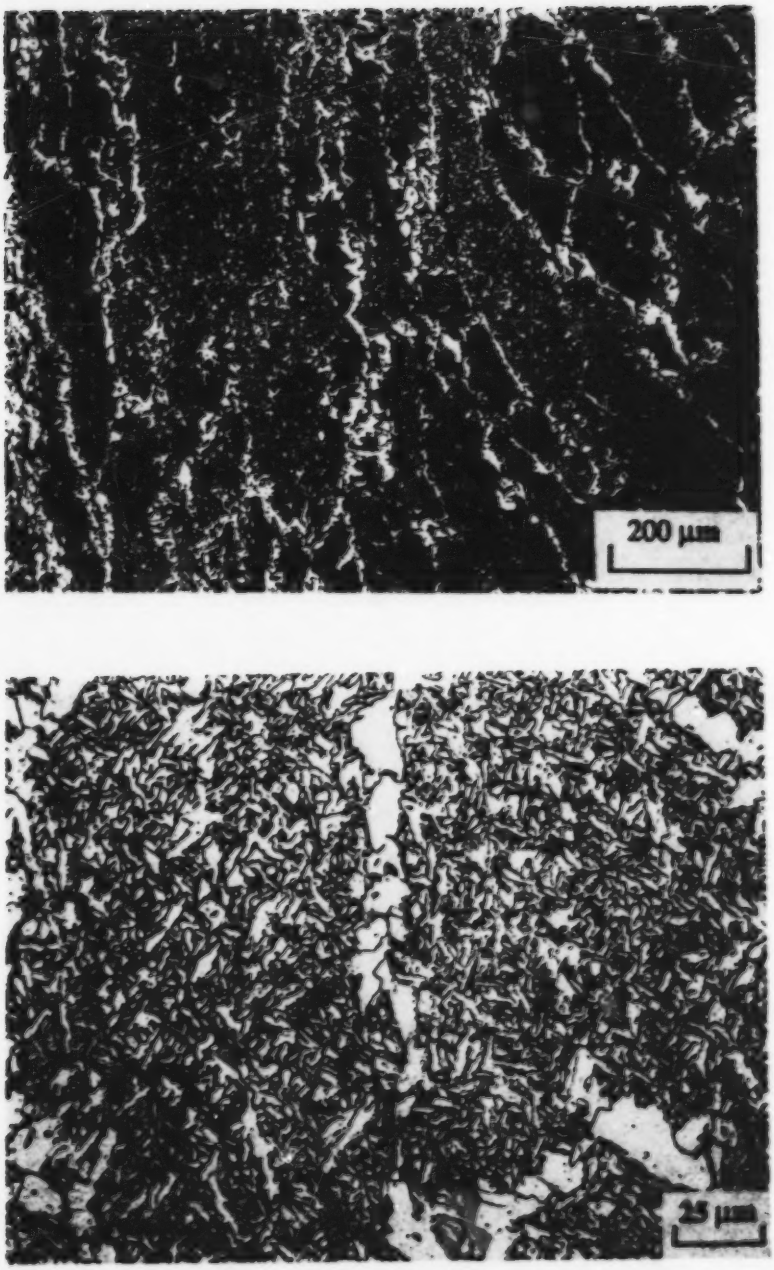

(c) Weld SA7 (neg.17537 and 17538)

Fig. 8 Microstructure of C-Mn-1% Ni as-deposited weld metals.

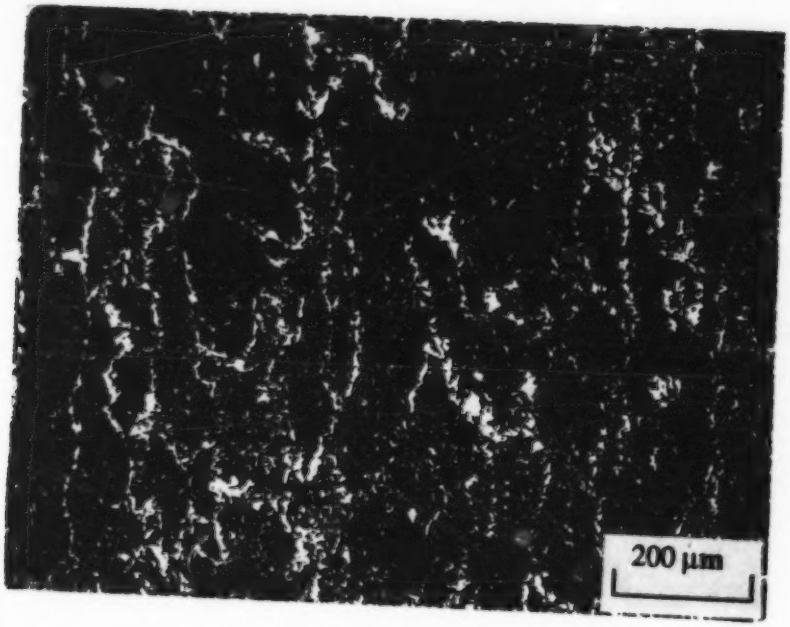

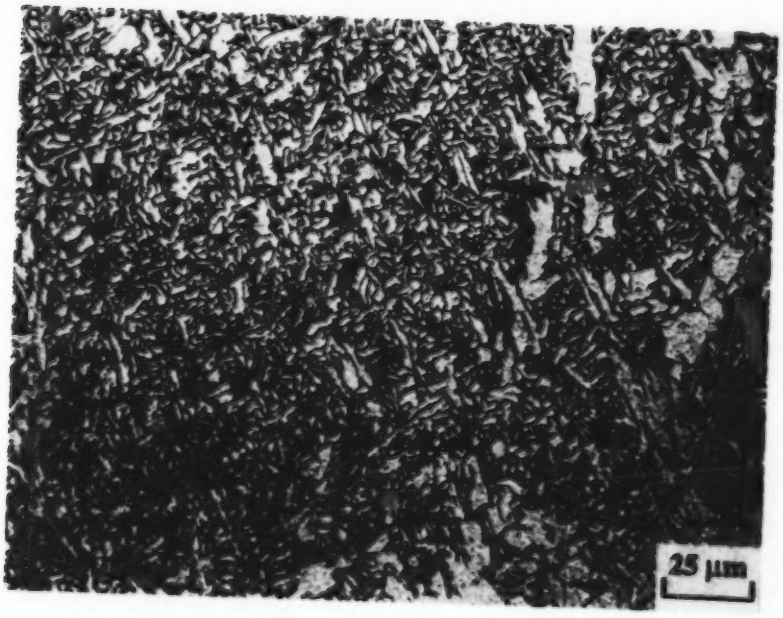

(a) Weld SA6 (neg.17539 and 17540)

Fig. 9 Cont'd

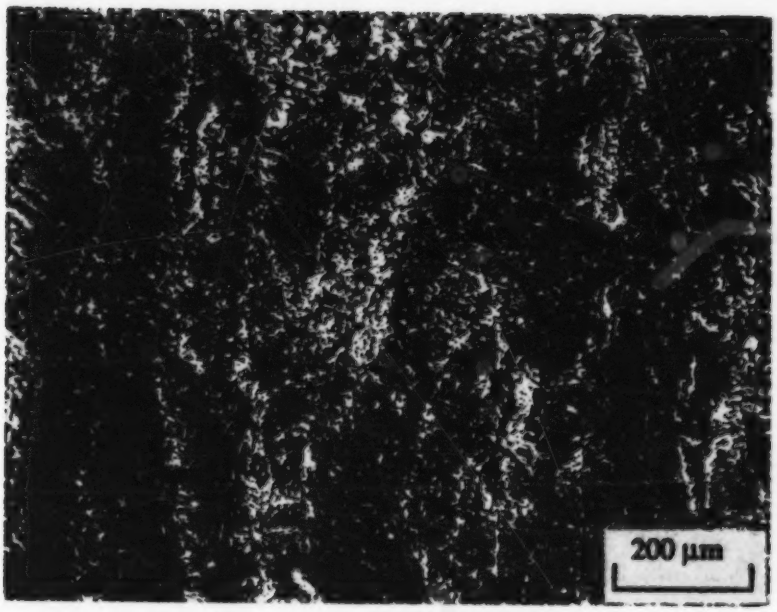

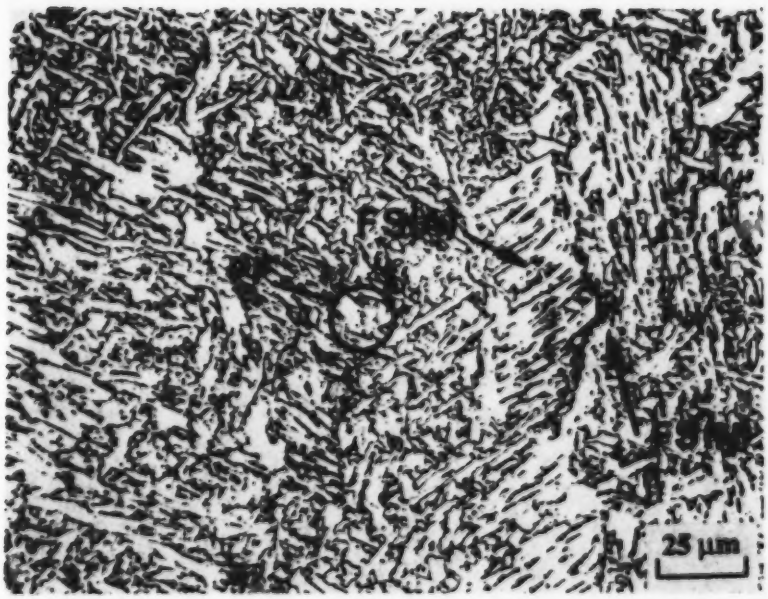

(b) Weld SA8 (neg.17541 and 17542)

Fig. 9 Microstructure of C-Mn-2-3% Ni as-deposited weld metals. Microconstituents: FS(A)-Ferrite with second phase (Aligned). FS(N)- Ferrite with second phase (Non-aligned) and PF- Polygonal Ferrite.

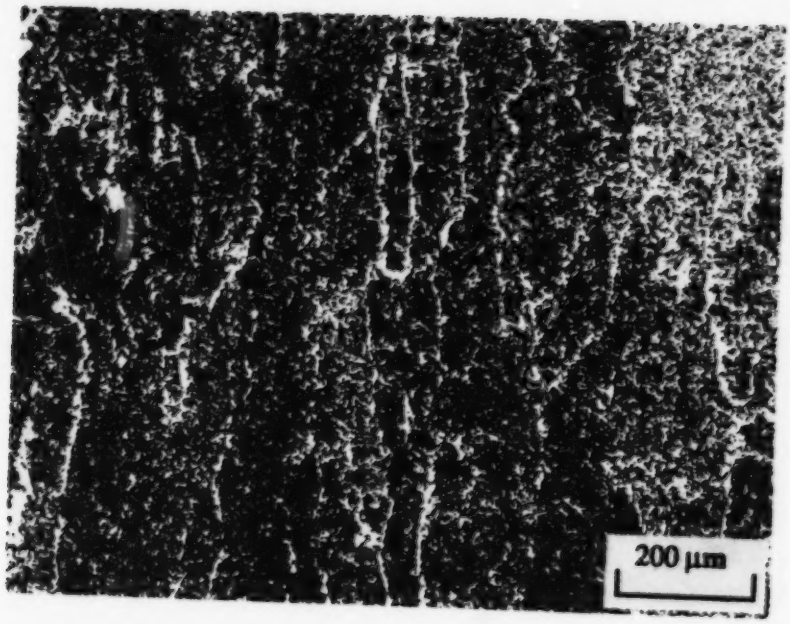

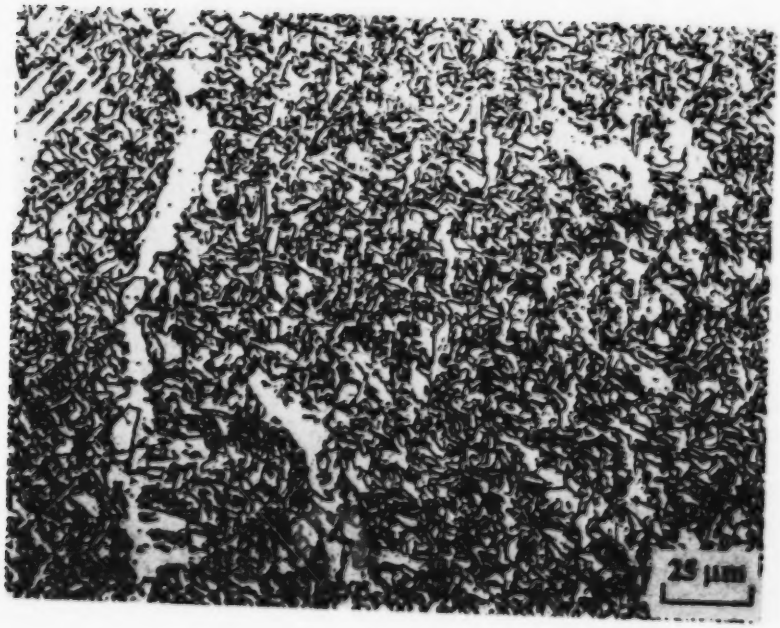

(a) Weld SA3 (neg.17543 and 17544)

Fig. 10 Cont'd

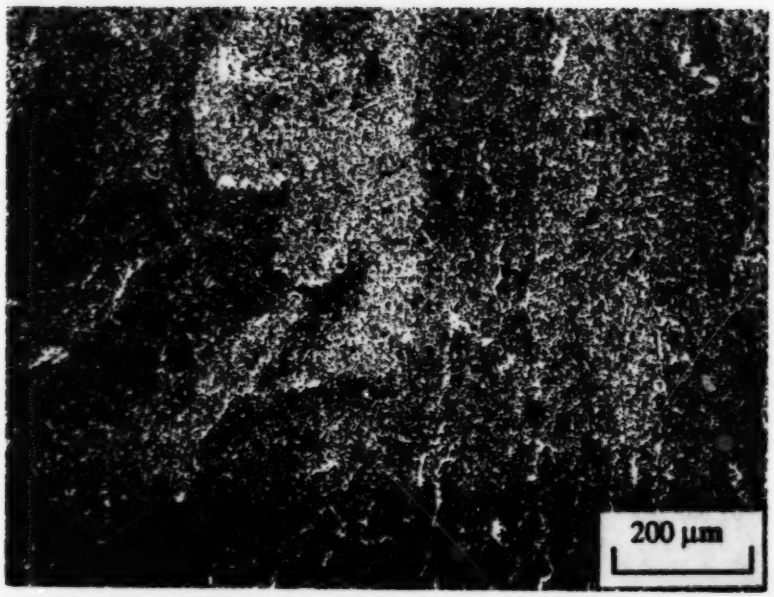

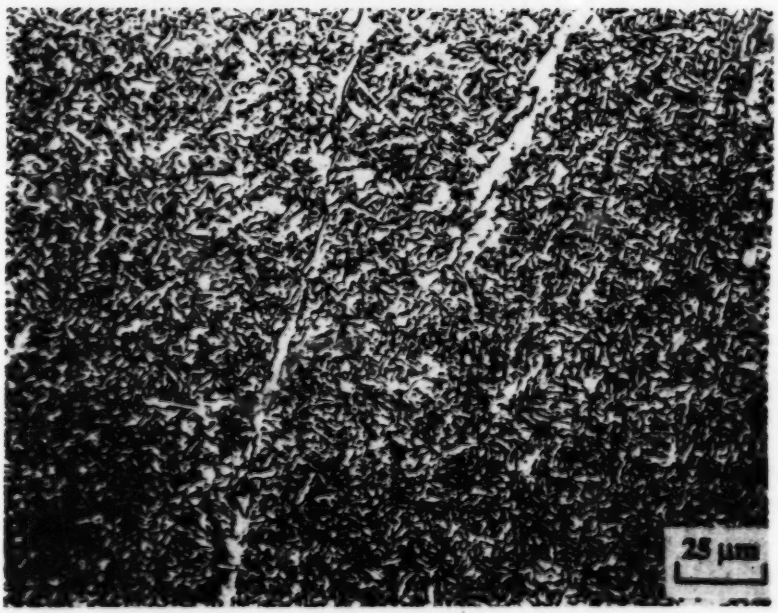

(b) Weld SA10 (neg.17545 and 17546)

Fig. 10 Cont'd

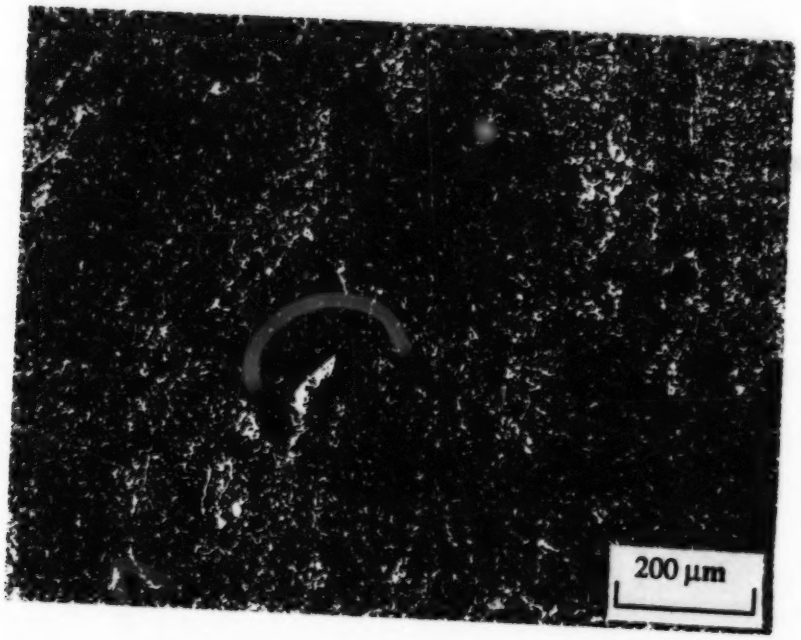

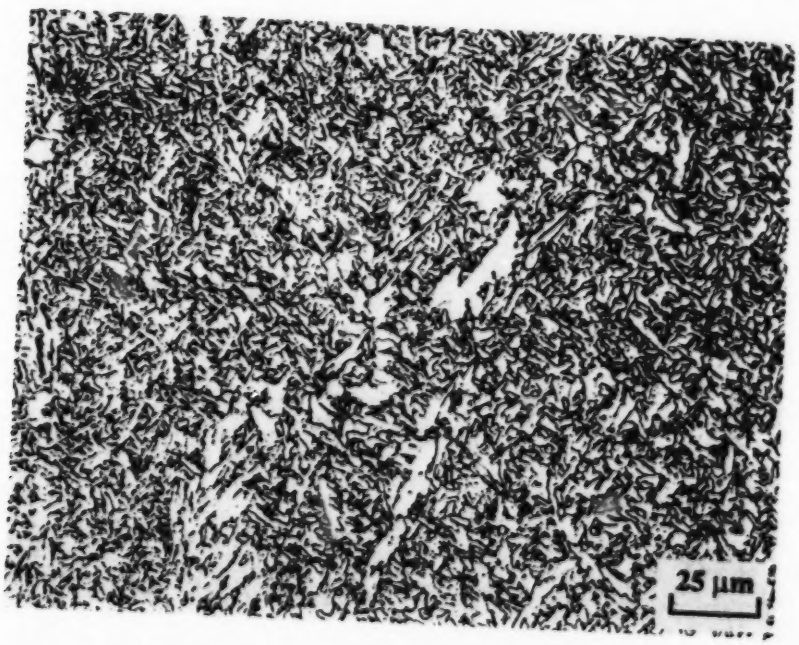

(c) Weld SA12 (neg.17547 and 17548)

Fig. 10 Microstructure of C-Mn-Ti-B and C-Mn-Mo as-deposited weld metals. Etch 2% Nital.

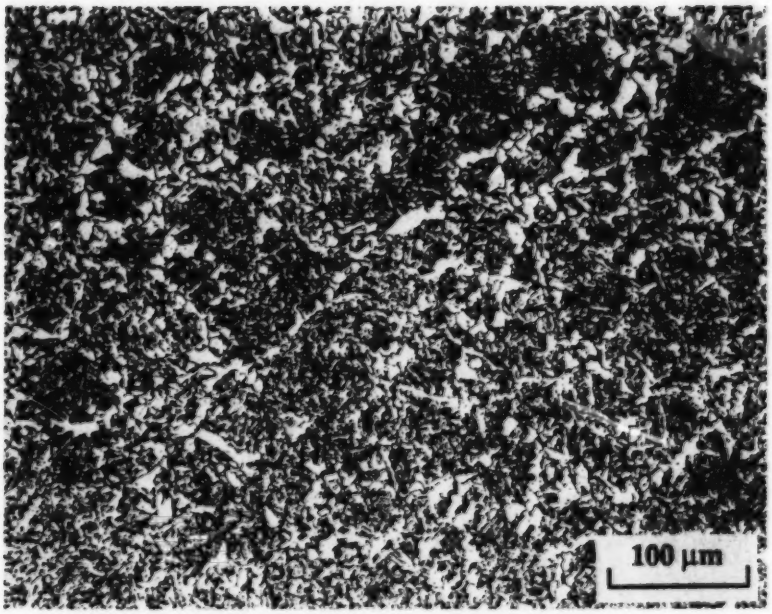

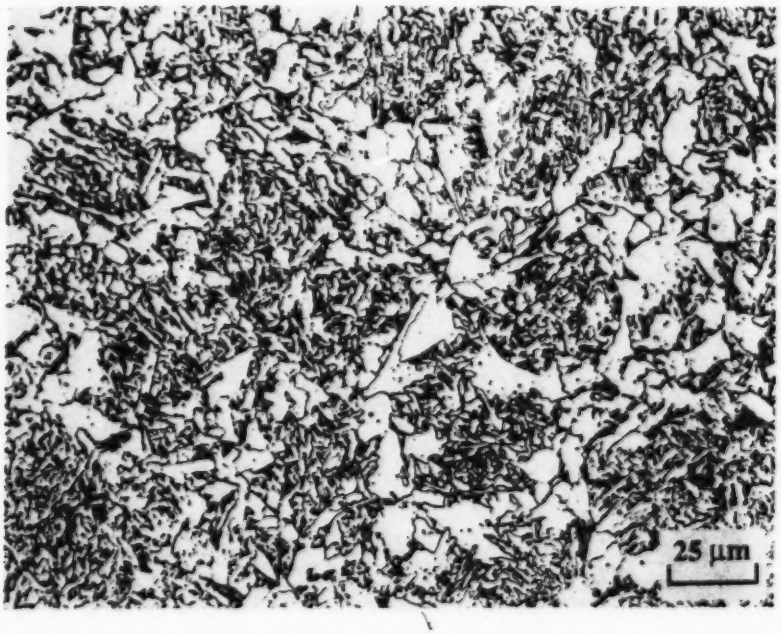

(a) Coarse grain reheated region (neg.17549 and 17550)

Fig. 11 Cont'd

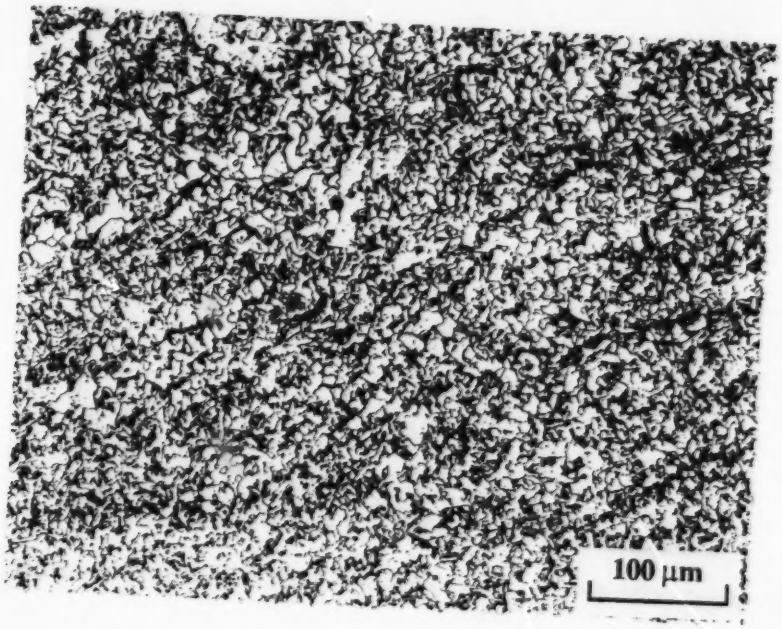

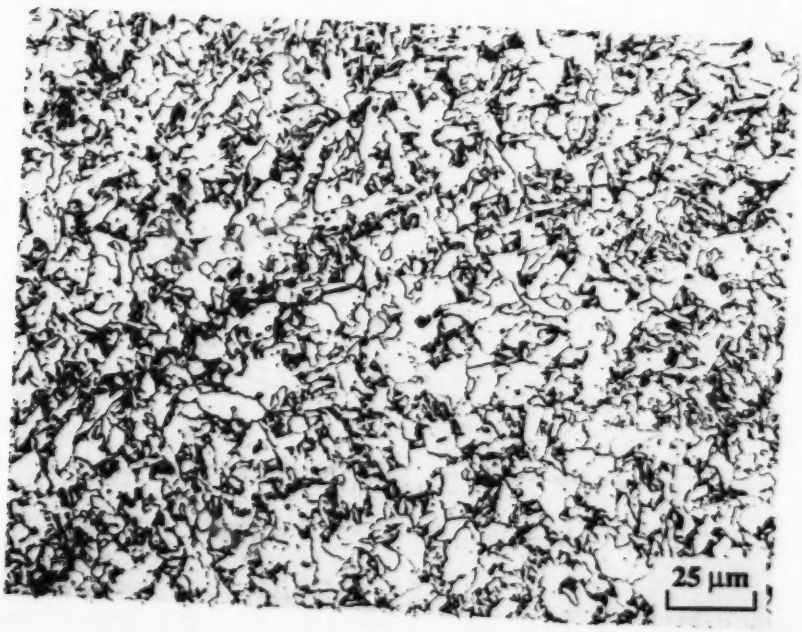

(b) Fine grain reheated region (neg.17551 and 17552)

Fig. 11 Typical microstructure of coarse grain and fine grain reheated weld metal regions.

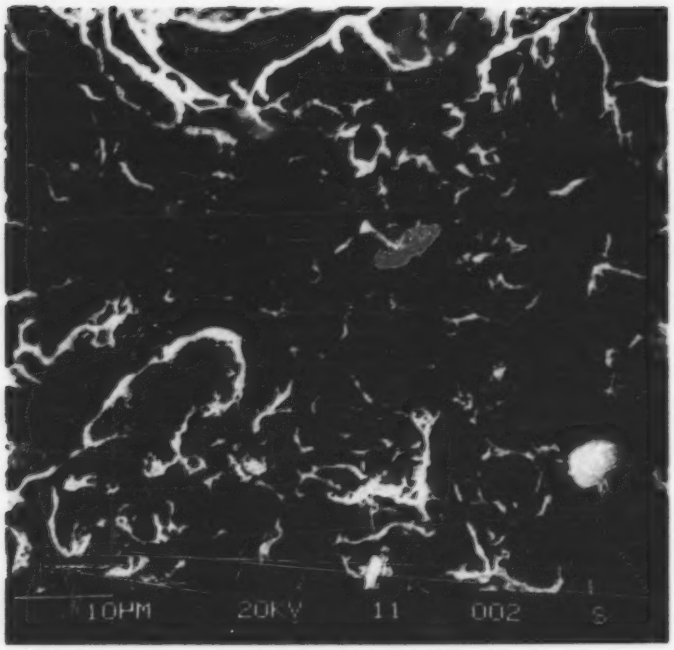

Fig. 12 Typical SEM fractograph showing initiation of cleavage failure from a large non-metallic inclusion. (neg. 35 mm).

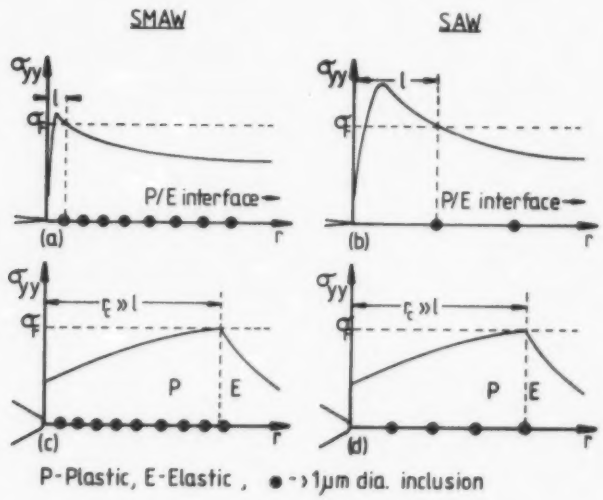

Fig. 13 Stress distribution as a function of distance, r, from sharp crack tip (a and b) and rounded notch (c and d). For sharp cracks, fracture occurs when the stress, σ_{yy}, exceeds the critical fracture stress, σ_F, over the distance " l ". For rounded notches, fracture occurs when the stress, σ_{yy}, reaches σ_F. (neg. 14032)